# RESULTS OF GEOELECTRIC MEASUREMENTS WITHIN THE OBI COAL DEPOSIT

BY

George Nnabuike Akubue B.Sc.

Thesis submitted to the Ahmadu Bello University in partial fulfilment of the requirements for the award of the degree of Master of Science

Department of Physics,
Ahmadu Bello University,
Zaria - N i g e r i a .

May 1977

# D E D I C A T I O N

THIS THESIS IS DEDICATED TO

MY WIFE AND CHILDREN

## A B S T R A C T

Results of Geoelectric measurements within Obi coal deposit show that the host rock which is shale has resistivity **ranging** from 5 to 14 ohm-m and within the shale exists a sub-section with resistivity from 15 to 30 ohm-m. Correlation with geological data reveals that this section contains the thick coal seams and is of the order of 60m **thick generally,**

Vertical electrical soundings (VES) have marked out the anticlinal structure within the area, and gave indications of three fault zones.

Self-potential measurements show one positive and one negative anomalies. While the negative anomaly is interpreted in terms of a fault zone the positive anomaly is attributed to an elevation effect.

Gravity measurements show that positive gravity anomalies exist over two fault zones in the area.

## A C K N O W L E D G E M E N T

I wish to express my gratitude to Mr. J.A. Adewumi, Head of Exploration N.S.D.A. who suggested this project and placed facilities for its execution at my disposal.

I am particularly grateful to Dr. D.E. Ajakaiye, Head of the Physics Department who in addition to her supervisory interest also made departmental equipments readily available. Her visit to me during the field trip was a source of encouragement. I also wish to thank Mr. S.B. Ojo and Mr. P.J.T. Verheijen for their supervisory interests too, useful suggestions on the project and patience in reading through the manuscript and draft.

My thanks goes to Mr. Famuboni and Mr. Aliu for their assistance in arranging equipment and transport for the field trip. It is necessary to thank Mr. B.J.O. Okafo, Mr. Odukwe, Mr. Okeudo, Mr. Oyeka, Dr. Boev and Mr. Migraev for their discussion and information on the geology of the Middle Benue.

I also wish to thank Mr. E. Oguike and D. Okoko for their assistance in the field work. I would like to thank my colleagues of Physics Department for their useful discussions during the final stages of this work.

Finally, I am indebted to the Nigerian Steel Development Authority for sponsoring me through this course.

Table of Contents


| | Page |
|---|---|
| Abstract .. .. .. .. .. .. | i |
| Acknowledgements .. .. .. .. .. | ii |
| Table of Contents .. .. .. .. | iii |
| List of Figures .. .. .. .. .. | vi |
| List of Tables .. .. .. .. .. | viii |
| List of Symbols .. .. .. .. .. | ix |
| Chapter I: INTRODUCTION .. .. .. | 1 |
| 1.1 General Introduction .. | 1 |
| 1.2 Previous geophysical work done in Obi area .. .. | 4 |
| 1.2.1 Resistivity work .. .. | 4 |
| 1.2.2 Gravity Work .. .. | 6 |
| 1.3 Geophysical work done in some other coal fields .. | 6 |
| 1.4 The Present Survey .. .. | 7 |
| Chapter II: GEOLOGY .. .. .. .. | 9 |
| 2.1 General Geology .. .. | 9 |
| 2.2 Local Geology .. .. | 11 |
| 2.3 Geological Structures .. | 16 |

| | | |
|---|---|---|
| Chapter III: | MODEL THEORETICAL RESISTIVITY CURVES FROM BOREHOLE DATA .. | 18 |
| | 3.1 Resistivity Logs and Computer procedure .. .. .. | 18 |
| | 3.2 Model resistivity curves | 21 |
| | 3.3 Results and deductions .. | 27 |
| Chapter IV: | ELECTRICAL RESISTIVITY SURVEY | 31 |
| | 4.1 General Field Procedures and Reduction of data .. | 31 |
| | 4.2 Interpretation of Sounding data | 36 |
| | 4.3 Resistivity Profiling .. | 50 |
| | 4.4 Limitations and error in the Resistivity Work .. | 62 |
| Chapter V: | SELF-POTENTIAL (SP) METHOD .. | 64 |
| | 5.1 The Origin of Self-Potential | 64 |
| | 5.2 Field Procedure and data reduction .. .. .. | 66 |
| | 5.3 Description and Interpretation of SP anomalies .. .. | 69 |
| Chapter VI: | GRAVITY METHOD .. .. .. | 78 |
| | 6.1 Field Work .. .. .. | 78 |
| | 6.2 Density Determination .. | 79 |
| | 6.3 Reduction of Data .. | 81 |
| | 6.4 Errors in Bouguer anomalies | 85 |
| | 6.5 Description and Interpretation of Bouguer anomalies .. | 86 |

Chapter VII: RESULTS AND CONCLUSIONS .. 95

7.1 Results from various methods 95

7.2 C o n c l u s i o n s .. 96

7.3 R e c o m m e n d a t i o n s 98

References: .. .. .. .. .. .. 99

Appendix: .. .. .. .. .. .. 102

1. Resistivity plots with electrode spread across the strike of the anticline.

List of Figures


| Fig No. | T i t l e | Page |
|---|---|---|
| 1.1 | Location of Obi area .. .. | 3 |
| 2.1 | Geological map of part of Middle Benue .. .. | 10 |
| 2.2 | Geological map of part of Lafia Coal deposit .. ..(in folder) | |
| 2.3 | Stratigraphic Scheme of the Cretaceous sediments in Lafia area | 13 |
| 3.1 | Model resistivity curve for a two-layer case .. .. | 22 |
| 3.2 (a,b) | Theoretical curves for boreholes 26 and 66 .. .. | 23 |
| 3.2 (c,d) | Theoretical curves for boreholes 96 and 45 .. .. | 24 |
| 3.3(a,b,c,d) | Model resistivity curves placing coal of thickness 3 m at various depths .. .. | 25-26 |
| 4.1 | Network of Profiles .. .. | 32 |
| 4.2 | Electrode configuration .. .. | 33 |
| 4.3 a | Interpretation of VES D and B curves | 38 |
| 4.3 b | Interpretation of VES A and E curves | 39 |
| 4.3 c | Interpretation of VES C and K curves | 40 |
| 4.4 a | Comparison of Geological and geoelectric sections for points A and B .. .. | 44 |
| 4.4 b | Comparison of geological and geoelectric sections for points D and E .. .. | 45 |

| | | |
|---|---|---|
| 4.5 | Interpretation of VES G curve .. | 47 |
| 4.6 | Geological section along profile VIII showing a fault .. .. | 48 |
| 4.7 a | Geoelectric section along DEF .. | 51 |
| 4.7 b | Simplified geological section along DEF .. .. | 52 |
| 4.7 c | Geoelectric section across ABC .. | 53 |
| 4.7 d | Geoelectric section across KEC .. | 54 |
| 4.8 | Profiling resistivity plots with 25 m electrode spacing .. .. | 57 |
| 4.9 | Profiling resistivity plots with 75 m electrode spacing .. .. | 58 |
| 4.10 | Contour map of resistivity values with 25 m electrode spacing .. | 59 |
| 4.11 | Contour map of resistivity values with 75 m electrode spacing .. | 60 |
| 5.1 | Plot of SP values corrected for topography .. .. | 68 |
| 5.2 | A sketch of the line currents likely to give rise to an SP anomaly .. | 71 |
| 5.3 a | SP anomaly 'C' and the model of the line charges .. .. | 74 |
| 5.3 b | SP anomaly 'A' and the model of line charges .. .. | 75 |
| 6.1 a | Bouguer anomaly along profile II | 87 |
| 6.1 b | Bouguer anomaly along profile V .. | 88 |
| 6.1 c | Bouguer anomaly along profile VIII | 89 |
| 6.2 | Two dimensional model for the anomaly SW of profile II .. .. | 90 |

## List of Tables


| Table | | Page |
|---|---|---|
| 2.1 | Stratigraphical Correlation .. .. | 12 |
| 3.1 | Resistivities and thicknesses of rock-types obtained from borehole logs | 20 |
| 4.1 | Geoelectric sections of interpretable VES curves .. .. | 41,42 |
| 6.1 | Densities of different rock-types in Obi coal deposit .. .. | 81 |

## LIST OF SYMBOLS

| Symbol | Meaning |
|---|---|
| m | Meter |
| km | Kilometer |
| $\Omega$ | Ohm |
| $\rho_a$ | Apparent resisti |
| N | North |
| NE | Northeast |
| SW | Southwest |
| E | East |
| mV | Millivolts |
| mA | Milliamps |
| cA | Centiamps |
| mgals | Milligals |
| S | Density |

# CHAPTER I

# I N T R O D U C T I O N

## 1.1 General Introduction

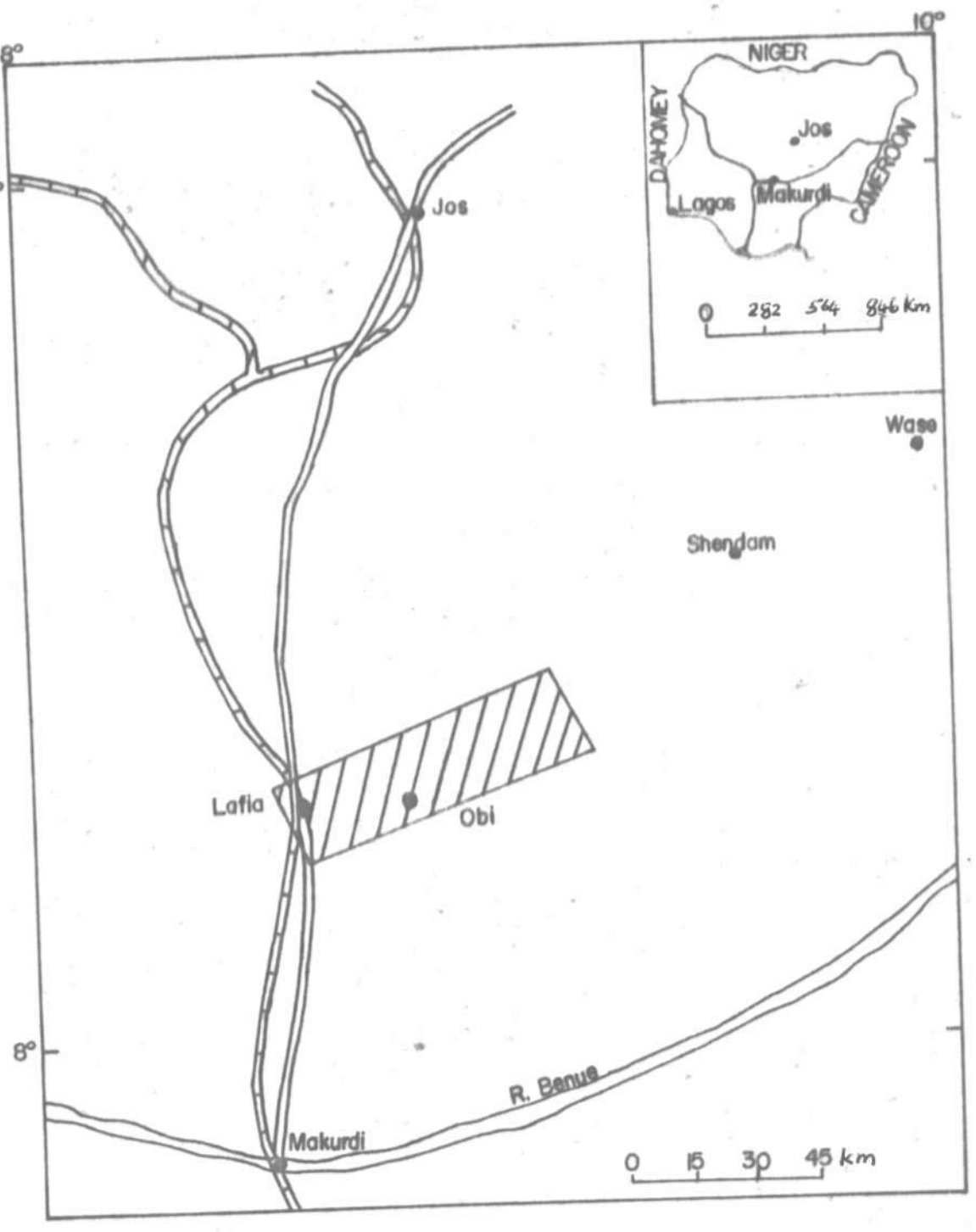
Coal mining in Nigeria dates back to 1915 when the Udi mine near Enugu in Anambra State was opened. Since then a lot has been achieved in the exploration and mining of coal in the country. Deposits were discovered in Ezimo and Inyi in the eastern, Kurukuruku in the western and Okaba in the Middle Belt of the country. The mined coal was in the first instance used as boiler fuel in locomotive engines by the Nigerian Railway Corporation (N.R.C.), in the generation of electricity by the then Electricity Corporation of Nigeria (now NEPA) and also for domestic purposes. These establishments have now almost discontinued with the use of coal as a source of fuel. All the known reserves are sub-bituminous and non-coking (De Swardt & Co., 1963).

Recently however, the Federal Government decided to establish an Iron and Steel Factory which will require tons of coking coal for its operation. It follows that a reasonable and exploitable reserve of such coal is highly desirable. Consequently, the Nigerian Steel Development Authority (N.S.D.A.) was established and

commissioned with the responsibility of exploring not only for iron ore but also for coking coal wherever possible in the country. A lot of work has been done by this body in this direction in some parts of the country especially around Lafia in Plateau State Nigeria **(Fig 1.1)**

The Obi area is part of the Lafia basin which has been under investigation by the N.S. D.A. for its coal reserve. This basin has been most widely covered by geological and drilling operations by N.S.D.A. Several coal seams have been identified by drilling and these vary in thicknesses, from about 0.2 m to 1.6 m, and to some extent differ in their other physical properties. Drilling results also suggest that there could be fault in addition to folding in the area.

As part of the exploratory effort, a geophysical survey using mainly direct current resistivity method was undertaken by the author during the months of November and December 1976, in the Obi coal zone. The survey was undertaken around the Giza anticline (Fig 2.1) where the coal seams are rather close to the surface (about 20 metres deep) according to drilling information. For most of the drillings




Lafia area prospected for coking coal by N.S.D.A.

Railway

Fig 1.1 Location of Obi area.

done initially, there was inadequate geological and geophysical control with the result that the operations have been very costly. For future drilling in the Benue trough, thorough control can be achieved by proper identification of coal zones by geophysical methods.

The main aim of the survey was therefore the identification of thick coal seams or other horizons associated with the coal by geophysical means. It was also hoped that identification of faulted zones would be possible as proper identification of such structures is vital in the planning of mining operations.

## 1.2 Previous geophysical work done in Obi area

### 1.2.1 Resistivity Work

Under contract 1717 signed between the Nigerian Steel Development Authority and a Soviet Geophysical Organisation 'TechnoExport', the electrical method of prospecting was employed by a team of Russian and Nigerian geophysicists on a regional scale in the then Lafia division of the former Benue/Plateau State. The work consisted principally of vertical sounding with the Schlumberger array. Most of the sounding points were located along the roads and pathways that were easily accessible. In addition, the interval

between the sounding points ranged between 05 and 2 km.

The result of the survey revealed three geoelectrical divisions corresponding to three rock complexes. These are:-

1. Igneous rocks with resistivity 200 - 5000 ohm-m
2. Sandstone with resistivity 20 - 20,000 ohm-m
3. Shale with resistivity 2 - 20 ohm-m (N.S.D.A. report 1974)

The shale was identified correctly as the main host rock for coal from borehole core samples.

The survey did not identify any coal seam, faults or fault lines in the present area of survey although the report suggested the existence of a lot of tectonic activity in the zone and recommended that at the stage of the detailed prospecting of coal-bearing areas, electrical prospecting could be of considerable help during mapping of tectonic faults and minor folds which complicated the structure of the coaly series. A current electrode spread of up to 1000 m was also recommended for the electrical soundings.

During the course of drilling, resistivity of the borehole sections was measured by using convetional logging techniques. The values obtained (table 3.1) provided

data for the model resistivity curves prepared prior to the present field work.

1.2.2 Gravity Work

Regional gravity survey had also been carried out in the area (Cratchley and Jones, 1965). Gravity stations were established at intervals of about 5 km on the accessible roads in the Benue valley. The Bouguer anomaly map placed Obi within a flat negative anomaly zone which was attributed to synclinal structures. Step faulted contacts within the area were also inferred especially on the northern side of the Benue trough from Lafia to Wase.

1.3 Geophysical Work Done in Some Other Coal Fields

Recent geophysical surveys carried out in some coal-fields in other countries showed encouraging results. An example of such is contained in a report on the geophysical survey over coal deposit in Creek, Central Queensland (Haber and Kopper, 1976). The results of their work showed that a resistivity anomaly and a positive self potential were measured over the known coal deposit. Also in India a gravity survey over Raniganj coal field (Verma et al, 1976) marked out the shale zone which was the host rock, but did not indicate individual coal seams.

1.4 The present survey

Borehole resistivity logs showed that reasonable resistivity contrasts exist between the various rock-types in the area. It is also known that vertical and dipping faults, beds and fissures can be detected by direct current prospecting methods (Van Norstrand, 1966). These facts suggested D.C. resistivity as a good method for achieving the aim of the survey listed under section 1.1....

The mineral content within a fault zone is most likely going to be different from that of adjacent non-faulted areas. Infiltration of fluids with salt concentrations into the fault zone can give rise to strong electrolytic effect which may result in self potential that differ from that of the surrounding. Self potential measurements can therefore give some insight into the existence of faults. Any difference in mineral composition of rocks will reflect on their densities and hence on the gravity measurements over areas bearing such rock-types. Self potential and gravity methods have therefore been included for possible identification of faults. These often show up on gravity maps too (Grant and West 1965).

One other useful method which could have been used was the seismic method. This method should trace out faults fairly distinctly and indicate the various strata since velocity contrast should exist between sandstone, shale and possibly coal. Although no velocity values were given for P-wave for the Benue strata, it is known that the P-wave velocity for shale in general ranges from 2300 $m\ s^{-1}$ to 5,000$ms^{-1}$ (Clark Jnr., 1966), and that of sandstone from about 1400 $m\ s^{-1}$ to 4,500 $m\ s^{-1}$ (Garland, 1971). Such velocity contrasts could easily be detected by the seismic method. However, only hammer seismic equipment was available and this was thought unsuitable to detect coal at depth of 20 m and below.

# CHAPTER II

# G E O L O G Y

## 2.1 General Geology

The Obi coalfield which is part of the Lafia Basin is located within the Benue trough. Although the geology of the trough is not yet fully understood, some general information has been provided by the work of Cratchley and Jones (1965) on one hand and the more recent one by Offodile (1976). Some more detailed information has also been available as a result of the extensive search for coking coal by the Nigerian Steel Development Authority in the study area. The Benue trough is divided into three main regions viz: the southwest, the middle Benue and the northeast.

The Lafia basin is assigned to the Middle Benue region (Cratchley and Jones, 1965) Fig 2.1. The stratigraphy is simple and dates from the Albian to the Maestrichtian. Quaternary deposits are scanty, unconsolidated and generally weathered (Okeudo, "personal communication").

The oldest sediments are the Asu River group lying unconformably on the crystalline rocks of the Precambrain basement. The Cenomanian stage is represented by the

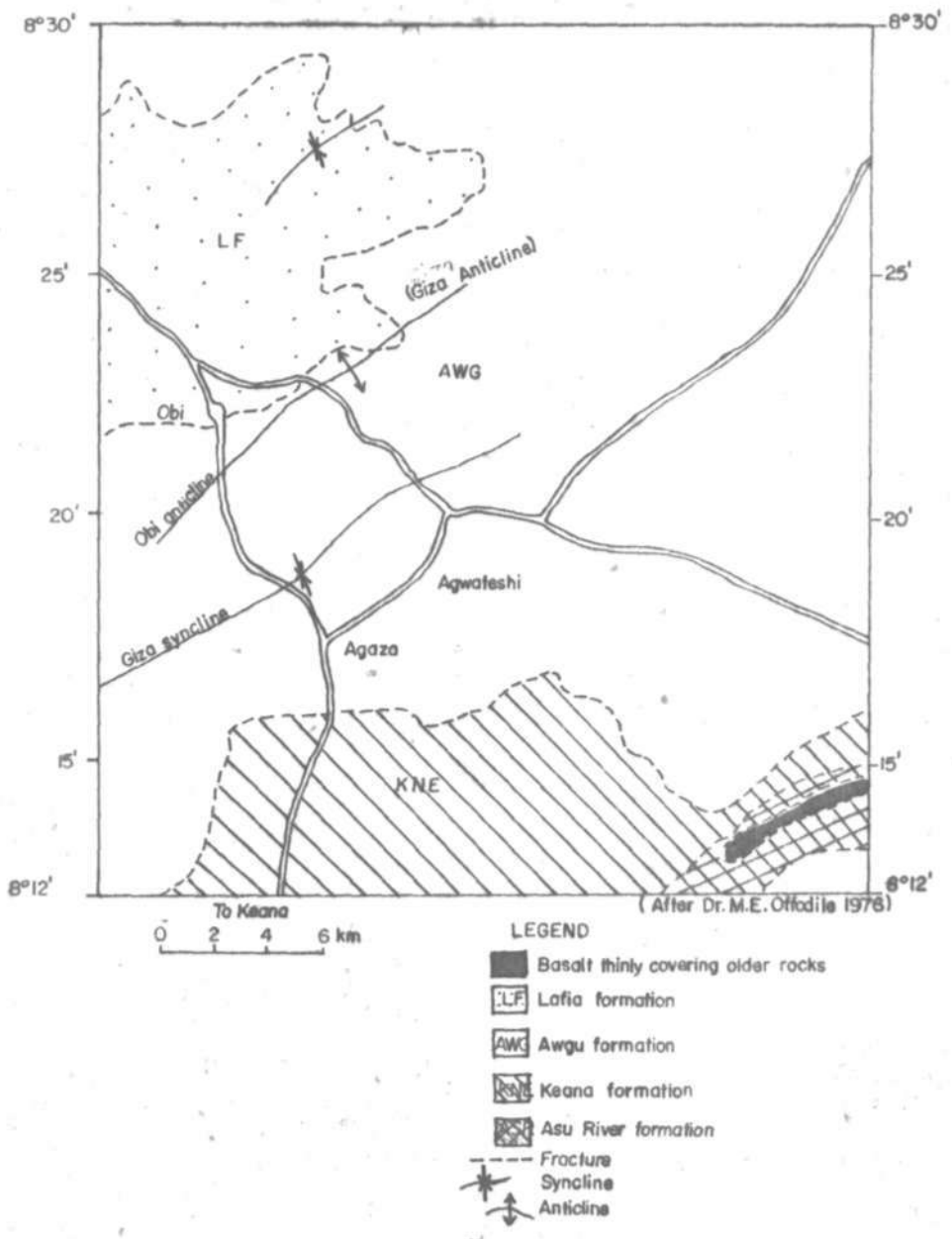



Fig 2.1 Geological map of part of Middle Benue

Keana sandstone, the transition deposits and the lower part of the marine deposits. The middle and upper parts of the marine deposits date from the Turonian to Senonian. The entire sequence is overlain by the Lafia sandstone Formation which was deposited between the upper Senonian and the Maestrichtian. These formations have been correlated with formations in other parts of the Benue trough and with other sedimentary basins in Nigeria (Cratchley and Jones, 1965; Offodile, 1976). The general stratigraphy is shown in Table 2.1.

## 2.2 Local Geology

The detailed study in the Obi area confirmed the usual cycle of sedimentation associated with coal basins (fig 2.2). This is a prominent character of the transition deposits in the Lafia basin (N.S.D.A., 1976). The stratigraphic scheme is shown in Fig 2.3 and a brief description of the lithologic units is as follows:

(i) The Precambrian Stage

This consists of granites, gneisses and pegmatites and their contact with the sedimentary cover has been detected to the north of Lafia.

TABLE 2.1

Stratigraphical Correlation

| Geological Stages | | South-West | Middle Benue | | North - East | |
|---|---|---|---|---|---|---|
| | | Oturkpo-Makurdi | Keana-Awe-Arufu | Bashar-Mari-Agar | Gombe | Lau |
| Maestrichtian | | Upper Coal Measures | Lafia Sandstone | Gombe Sandstone | Gombe Sandstone | Lamja Sandstone |
| | | False-bedded Sandstone | | | | |
| | | Lower Coal Measures | | | | Numanha Shale |
| Senonian | Campanian | Enugu-Nkporo-Shales | Marine deposits | Kumberi Formation | Pindiga Formation | Sekule Formation |
| | Santonian | ? ? ? | | | | |
| | Coniacian | Awgu-Shales | | | | Jessu Formation |
| TURONIAN | | Eze-Aku Shales / Makurdi Sandstone | | | | Dukul Formation |
| CENOMANIAN | | | transition deposits | Passage beds | Yolde Formation | Yolde Formation |
| | | | Keana sandstone | Muri Sandstone | Bima Sandstone | Bima Sandstone |
| ALBIAN | | Asu River Group | Asu River Group | Marine deposit | | Marine deposits |
| PALAEOZOIC AND PRE CAMBRIAN | | Crystalline basement | | | | |

After Cratchley and Jones 1963

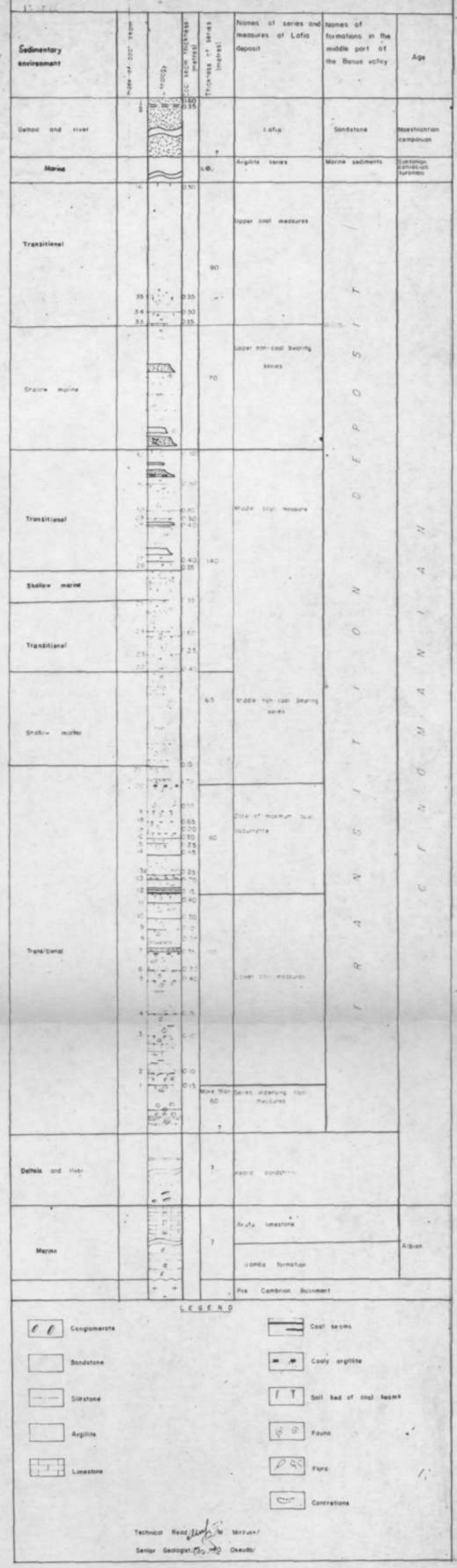
33⅓ Reduction

Enclosure No 4

NSDA
CONTRACT 1717.

# STRATIGRAPHIC SCHEME
## OF THE CRETACEOUS SEDIMENTS
## LAFIA DEPOSIT AREA

SCALE 1:3000



(ii) Cretaceous Stage

The Precambrian is overlain by the Upper Cretaceous with a total sedimentary thickness of about 1.2 km and contains in order of deposition;

(a) the Keana sandstone which is found south of Obi coalfield.

(b) the series underlying coalmeasures which contains carbonates, sandstones, shales, siltstones, limestones and occasional beds of carbonaceous shale.

(c) the lower coalmeasures which is rich in shale with imprints of charred flora. A few coal seams are associated with these measures which has thickness of up to 100 m.

(d) the measures of maximum coal content with a thickness of about 60 - 65 m. It consists mainly of intercalating beds of shale, sandstone, siltstone and coal. Among the coal beds revealed by drilling in this measures are those designated as

seams 12 and 13 have been described as the most economical in the area (N.S.D.A., 1974)

(e) the coal free zone which overlies (d) above with a thickness of about 90 m and made up of shale and considerable amount of carbonaceous material and clayey limestone.

(f) the upper coal measures which is similar to (e) but is about 300 m thick.

(g) shale series with average thickness of about 300 - 350 m which consists of dark grey shales with fragments of fauna and small amount of charred flora. In some places it contains coal. The series is related to the "marine facies" marked out by Reyment (Reyment, 1963) with underlying series corresponding to the transition deposits which have sustained considerable tectonic activities.

(h) the Lafia sandstone which contains sandstone of various grain size intercalating with beds of shale, siltstones and sometimes thin coal seams.

(iii) The Tertiary and quarternary series.

These form the youngest deposits and consist of poorly lithified grey and light grey clayish schists above basalt series. Sand and clay occur mainly along streams and river valleys.

Within the project area it is likely that the series of maximum coal content described above is next to the Quarternary deposit, with the Lafia sandstone and the underlying series down to the coal free zone being absent.

## 2.3 Geological Structures

The complex structure of the area under study can be related on a regional scale to the structural development of the Benue trough in which it is situated. The Benue graben is the primary tectonic structure which was the initial depression that received the Late Cretaceous sediments which later suffered a lot of tectonic upheavals. The trough (graben) is characterised by SW-NE trending regional folds that are parallel to the general trend of the Benue graben.

The Obi and Giza folds in the Obi area are only a part of these. The Obi syncline in the north and the Giza syncline in the south are separated by the Giza anticline (Fig 2.1). The present survey is almost on the crest of the Giza anticline which together with the synclines trend SW - NE, following the general strike of the Benue graben. In addition, the area is intensely faulted. Within the small Obi area for instance in Fig 2.2 many reverse and normal faults have been inferred (N.S.D.A., 1976). Most of these faults trend almost E - W. It is not obvious whether only E. - W faults exist, or that N - S trending faults may also exist.

# CHAPTER III

## MODEL THEORETICAL CURVES FROM BOREHOLE DATA

### 3.1 Resistivity logs and computer procedure

As stated in section 1.2 resistivity borehole logs were obtained from the area using the conventional methods. These were the normal device and the lateral device. The normal device gave a better picture of the resistivities of the formations than the lateral device. This is because in general the resistivity log from the former is symmetrical about the individual beds being scanned and the peak value corresponds nearly to the resistivity of the formation. Logs from this device also showed very good resolution especially in marking out the coal beds from the shale. Sandstone beds were also indicated except for the limitations which will be discussed below. The range of resistivities and thicknesses of the various rock types is given in table 3.1.

The logs showed good resistivity contrast between the host rock which is mainly shale and the other rock-types like coal, sandstone, and limestone beds. There was however, no definite contrast between the coal seams and sandstone beds where both occur, as their resistivities are

of the same order of magnitude in most of the boreholes.

A table of geologic sections and corresponding resistivity values was compiled and using a computer programme, theoretical curves were plotted using the parameters from each of eight boreholes. The parameters are indicated at the top left hand corner of the curves (Fig 3.1, 3.2).

The computer programme is based on a method developed by Johansen (1975) and written for the Department of Physics' HP 9830 A mini-computer and plotter (Verheijen, personal communication). The method consists of three main stages:

(i) A guess of the layer parameters ($\rho_i$ , $d_i$) is made from the operators knowledge of the area where $\rho_i$ , $d_i$ are the resistivity and thickness respectively.

(ii) the resistivity Transform of ($\rho_i$ , $d_i$) is calculated and the apparent resistivity $\rho_{app}$ ($\rho_i$ , $d_i$) found by convolution with the filter coefficients.

Table 3.1

Different rock types and their range of resistivity values obtained from borehole logs in Obi coal field.

| Rock type | Resistivities ohm-m | Thicknesses in m |
|---|---|---|
| Top clay | over 200 | 5 m assumed |
| Shale | 5 - 10 | 0.15 - over 40 |
| Coal | 25 - 70 | 0.1 - 2 |
| Sandstone | 30 - 70 | 0.2 - 10 |
| Limestone | 10 - 50 | 0.1 - 0.5 |
| Shale inter-calation with c o a l | 5 - 15 | 0.1 - 5 m |

(iii) ($\rho_i$ , $d_i$) are adjusted by trial and error until $\rho_{app}$ - curve agrees with the measured data.
In constructing the model curves however, step (iii) above is omitted since true borehole sections (thicknesses and resistivities) are being used.

Johansen tested the precision of the filter and showed that the error between $\rho_{conv}$ as calculated from the transform and $\rho_{exact}$ calculated from exact formula is less than $10^{-6}$.

3.2 Model Curves

In plotting the model curves three approaches were adopted:-

(a) A curve comprising two layers was constructed consisting of only the overburden with a thickness of 5 m and resistivity of 200 ohm-m and shale with resistivity 8 ohm-m.

(b) Actual resistivity values and thicknesses of the layers were then fed into the computer. Beds of the order of 0.5 m thick were neglected and horizontal layering was assumed. This meant that

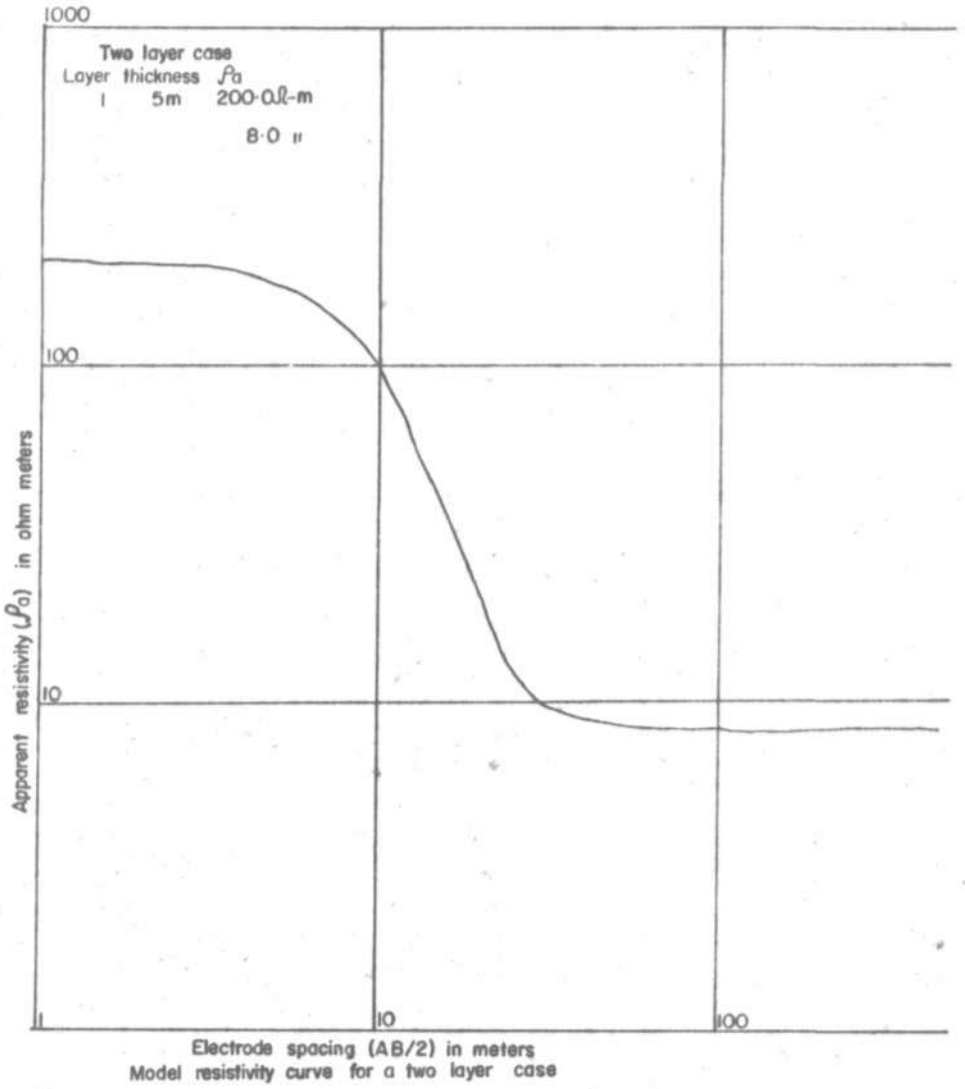



Fig 3.1 Model resistivity curve for a two layer case

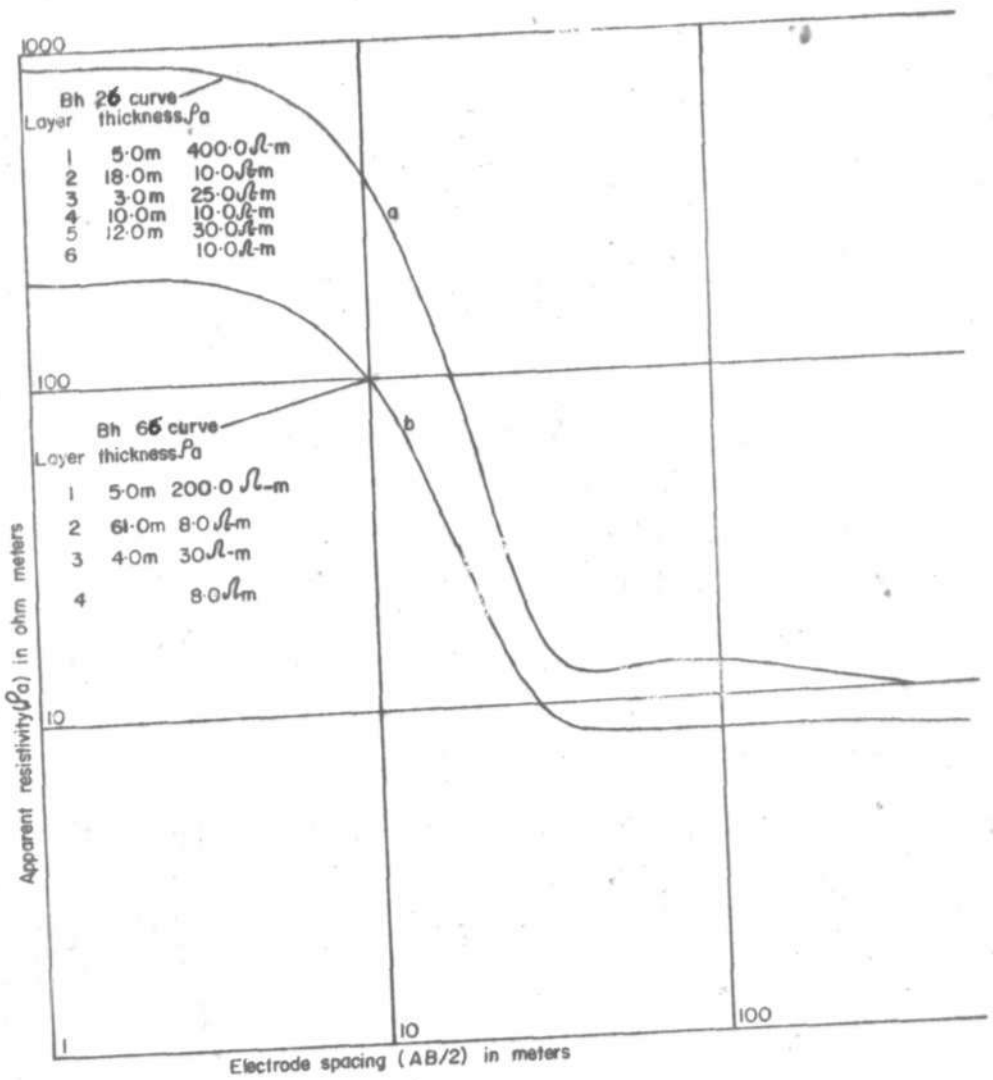



Fig. 3.2 (a.b) Theoretical curves for boreholes 26 and 66

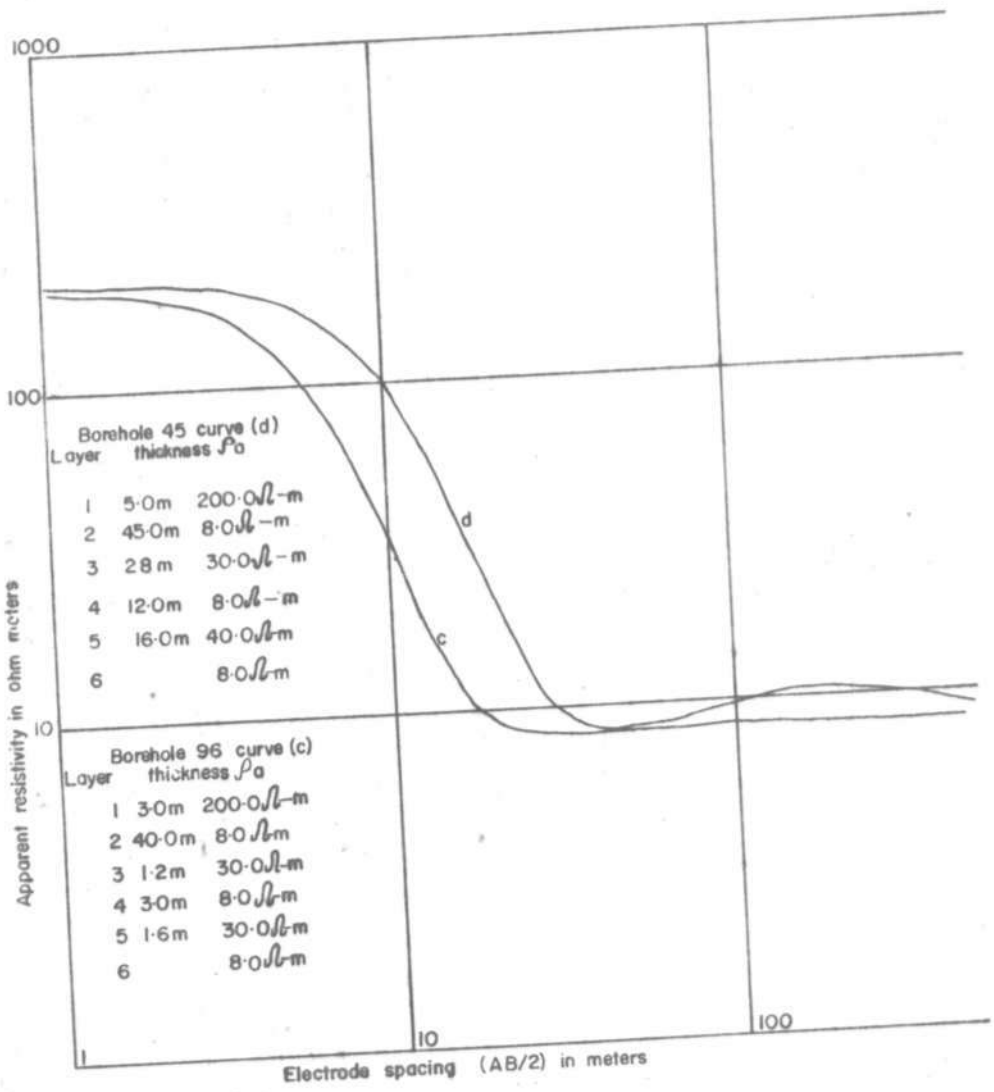



Fig. 3.2 (c,d) Theoretical curves for boreholes 96 and 45

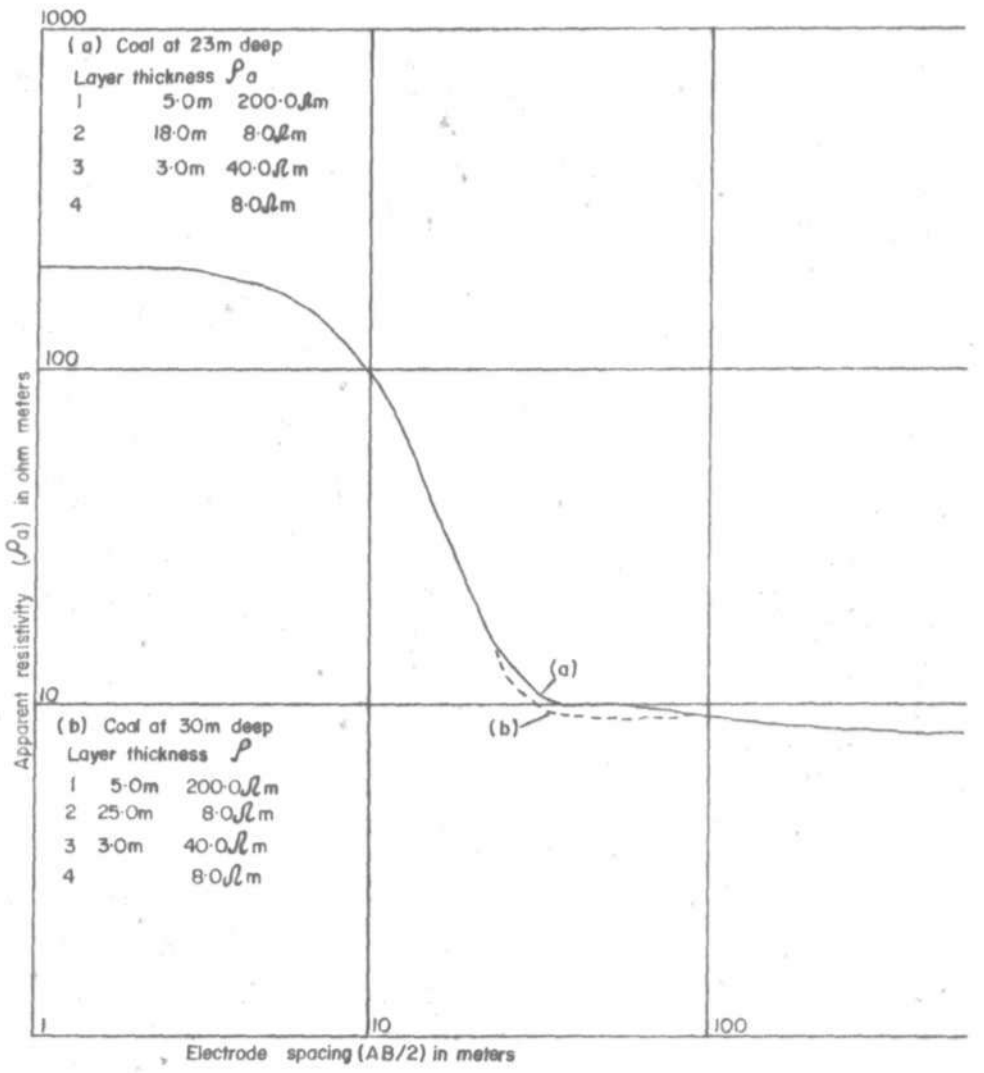



Fig. 3.3 (a,b) Model resistivity curves placing coal of thickness 3 m at various depths.

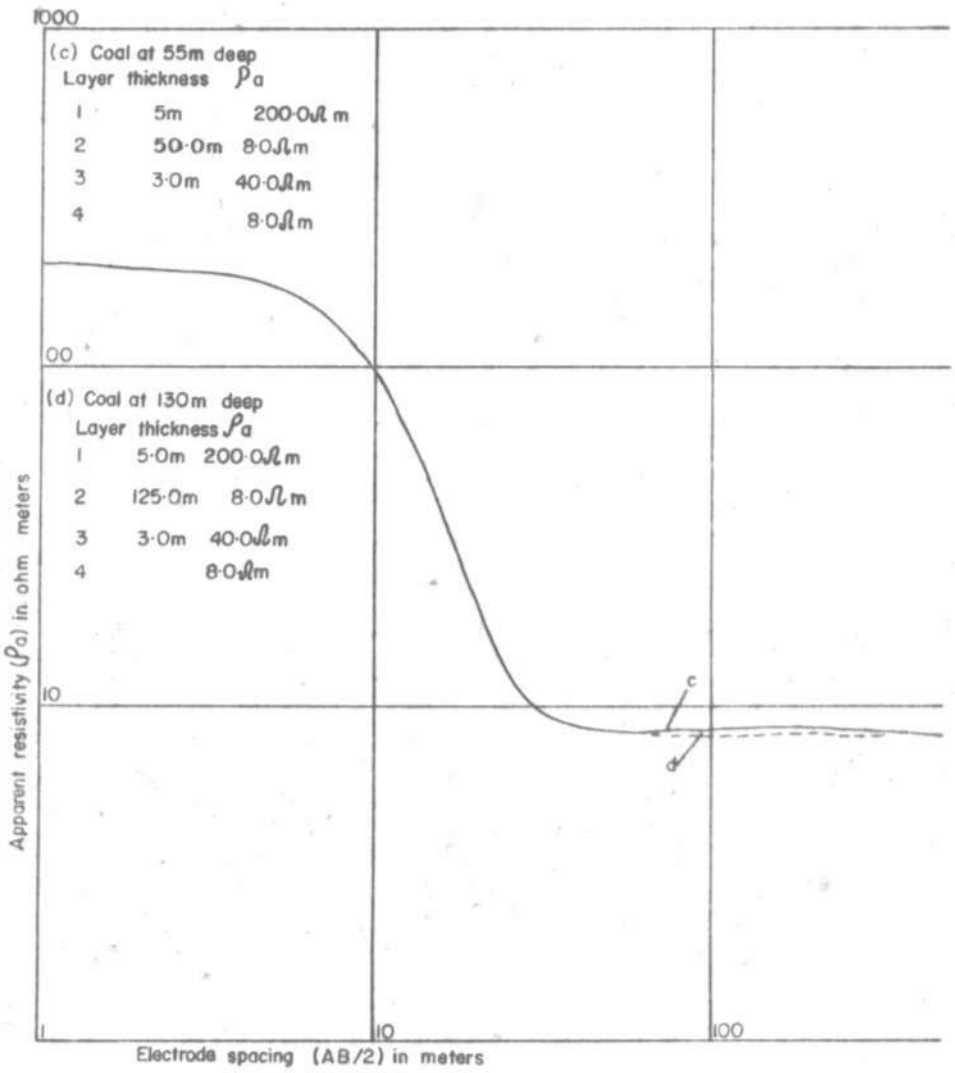



Fig. 3.3 (c,d) Model resistivity curves placing coal of thickness 3 m at various depths

the number of layers was approximated to what could be regarded as reasonable for a particular borehole. As this appeared subjective various combinations of the layer thicknesses were used to determine the effect of the approximations from the general shape of the curves. Layers that did not contribute to the overall shape were neglected.

(c) The coal seam of thickness 3 m and resistivity 40 ohm-m was placed at various depths within shale of resistivity 8 ohm-m assuming the absence of any other rock-type.

The three cases were then considered and compared. Representative curves are shown in Fig 3.1, Fig 3.2 (a,b,c,d) and Fig 3.3 (a,b,c,d).

3.3 Results and Deductions

(i) The shale zone was clearly indicated in the absence of any other rock type Fig 3.1.

(ii) The introduction of a thick bed of coal about 4 m thick did not alter the nature of the curve appreciably (Fig 3.2, b,c).

(iii) Wherever coal and sandstone and any other bed with resistivity greater than that of shale occurred together, a well defined anomaly was indicated within the shale zone Fig 3.2d.

(iv) Fig 3.2d also showed that suppression effect could be expected. Suppression effect often occurs when for instance a thin bed of low resistivity sandwiched between two beds of high resistivity is not shown in the resistivity curve. This means that the presence of such a bed does not affect the nature of the curve and cannot therefore be easily recognised in interpretation.

(v) From the second approach it could be seen that for coal with resistivity 40 ohm-m there was fairly good resolution between the overburden and shale on one hand and between shale and coal on the other Fig 3.3 (a,b). This resolution was better for coal seam that is fairly shallow and of the order of 30 m deep.

(vi) The resolution became less distinct as the depth of coal was increased, for instance in Fig 3.3c where the coal was about 50 m deep.

(vii) Beyond a depth of about 70 m there was no indication of the presence of any coal seam within the shale host rock. The situation, thus approximated a simple two layer case (Fig 3.3 d).

From the above results two obvious deductions could be made. The poor resolution existing between coal and shale meant that very careful and accurate measurement would be required if the coal was to be detected at all from electrical sounding data. Also the poor resistivity contrast between coal and sandstone could lead to erroneous interpretation. However, whenever the two occurred together it was conspicuously shown on the resistivity curve. Another consideration is that in preparing the model curves constant resistivity value had been used for a particular rock type in the area. This would not be strictly true in a real situation. Well logging gave the range of the resistivity of coal as lying between 25 to 50 ohm-m while the resistivity of

# CHAPTER IV

# ELECTRICAL RESISTIVITY SURVEY

## 4.1 General Field Procedures and Data Reduction

A Russian-made "Electronic indicating compensator" model )( K-I was employed in this survey for resistivity measurements. It consists of a meter used for measuring both voltage and current. Steel electrodes and copper electrodes were used as current and potential electrodes respectively. The meter reads to an accuracy of 0.01 centiamps or volt and its caliberation with standard meters show that it has an error of not more than 2% on all the scale ranges used in current and voltage measurements.

Seven profiles running approximately NE - SW following the general strike of the rock types were laid out as shown in Fig 4.1 and Fig 2.2. Each profile is about 900 meters long and the distance separating the two outermost profiles is about 1 km. Thus the survey covered an area of almost 1 sq km.

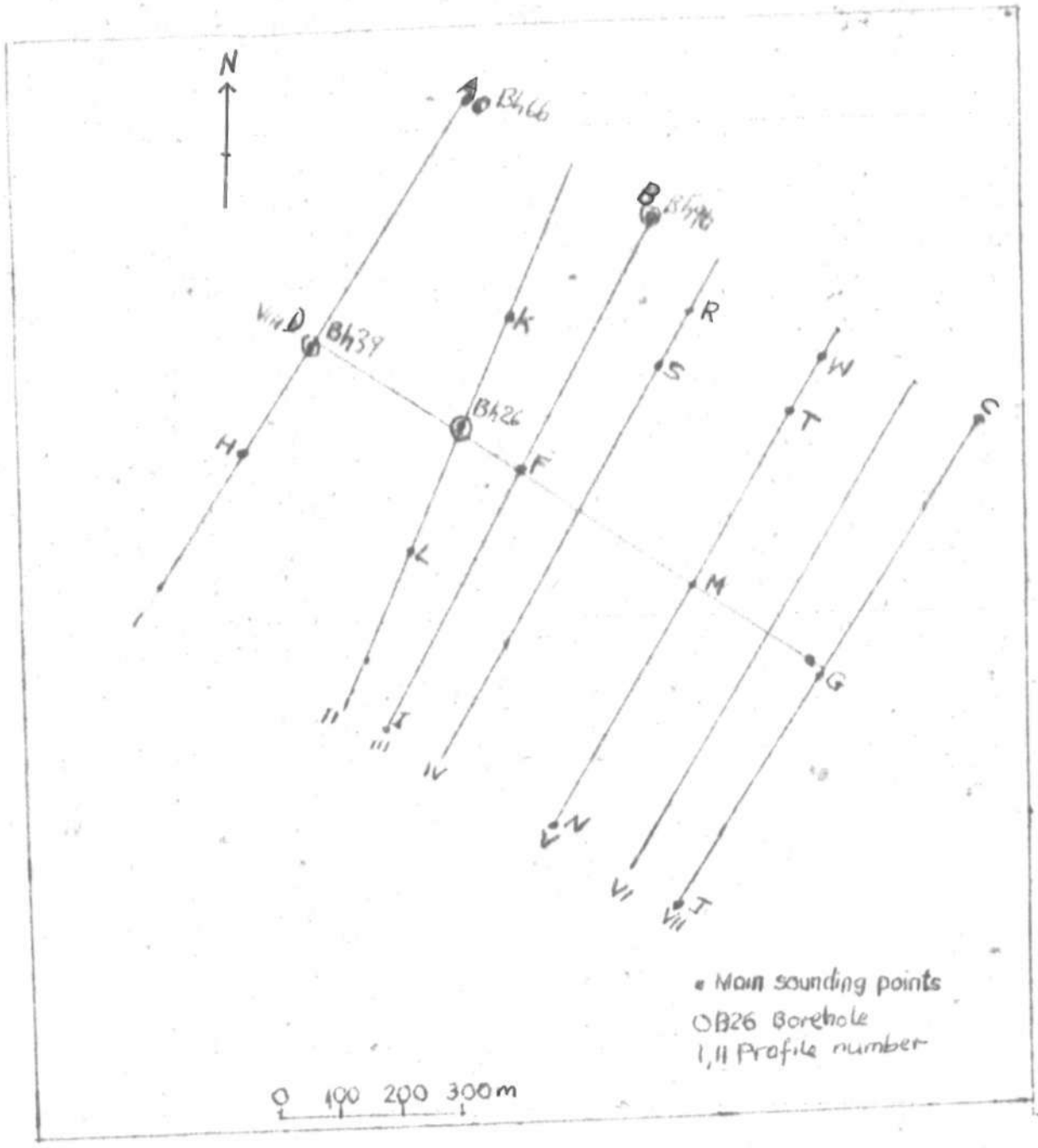



Fig. 4.1 Network of Profiles

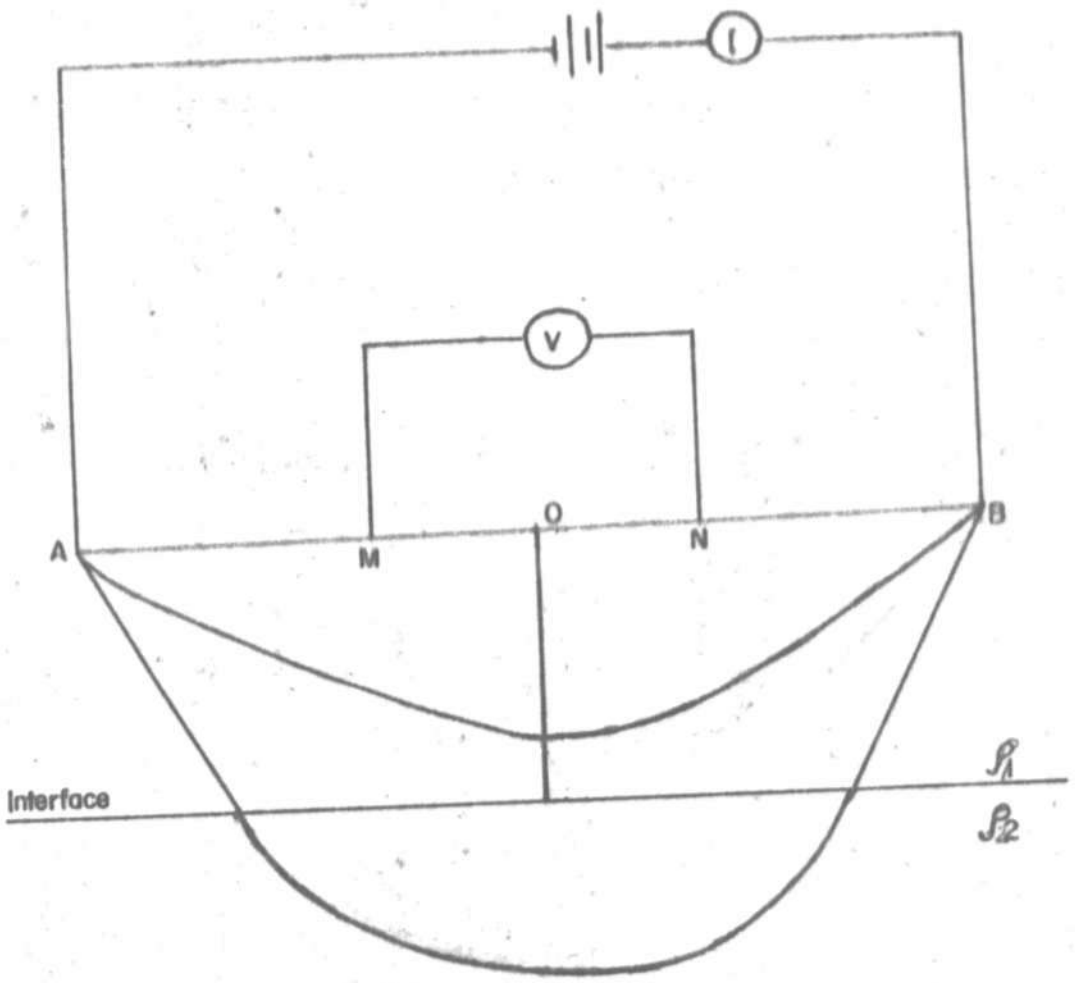



Fig 4.2 Electrode configuration

The Schlumberger electrode configuration was adopted in making vertical electrical soundings. The current electrode spread was between 600 m and 1000 m. The electrode configuration was first oriented across the anticline at points A,B,E,I, and D. The curves obtained were irregular and difficult to interprete (Appendix I). With the configuration running parallel to the strike of the anticline the curves obtained were more regular and similar to the model curves obtained with borehole data at A, and B (Fig 3.2). Hence the Schlumberger electrode configuration oriented parallel to the general strike of the anticline was employed in sounding at further points C,F,G,H,J,K,L,M, and N. Most of the curves obtained from these points resemble the model curves derived in Chapter III and confirm that the orientation chosen is reasonable. The soundings at A,B,D, and E, located close to boreholes were done in order to facilitate comparisons with results from well logs.

For each sounding point the potential electrodes M and N (Fig 4.2) were separated by distances raning from 0.66 m to 150 m while the current electrodes A and B were separated by 2 m to 1000 m and sometimes only up to 600 m when it was not possible to obtain readings at 1000 m.

The potential electrode spacing was maintained such that it was never more than 1/5 the current spread. Whenever the drop was too small to be measured, the potential electrodes separation was increased and measurements repeated in order to get overlapping readings for a change-over of MN from one value to the other. From the field curves it was noticed that this change-over led to a shifting in most of the curves but since such shifting was generally never high it was only necessary to apply visual smoothing. This type of correction may affect slightly the value of the resistivity but not the layer thicknesses (Zohdy et al, 1973; Van Norstrand, 1966).

Voltage drops across the potential electrodes were measured in millivolts (mV) while the transmitted current was measured in centiamps (cA). The field readings ranged from 0.01 to a few hundred millivolts and 0.2 cA to nearly 4 cA. Apparent resistivities were calculated using the formula

$$\rho_a = \frac{\Pi L^2 V}{2\ell I} \qquad \text{(Parasnis 1975)}$$

where $\rho_a$ is the Schlumberger apparent resistivity, L half the current electrode spacing and I equals the amount of

Representative curves are shown in Fig 4.3 (a,b,c,). Table 4.1 shows the results obtained from the curves corresponding to the sounding points.

The results of the interpretable resistivity sounding curves show a multi-layer geological structure in the area. The simplest are three layer situations and in other instances accurate curve matching and computer calculations show up to five-layer cases. From all the points the overburden resistivity appears to range from over 200 ohm-m to nearly 3000 ohm-m with a thickness varying from 1 m to over 6 m. The beds below the overburden are much more conductive and fall into three principal categories. The first has resistivity ranging from 6.5 ohm-m (Point A) to about 10 ohm-m (Point E) while the second has resistivity varying from over 10 ohm-m (Point B) to nearly 30 ohm-m (Point E). The third has resistivity similar to the first. At some points, geoelectric sections with resistivities varying from 30 ohm-m (Point A) to 300 ohm-m (Point E) are indicated just below the high resistivity overburden. At such points the overburden is thicker than what is given for the first layer. The predominant section is however the very low resistivity type and is likely to represent the

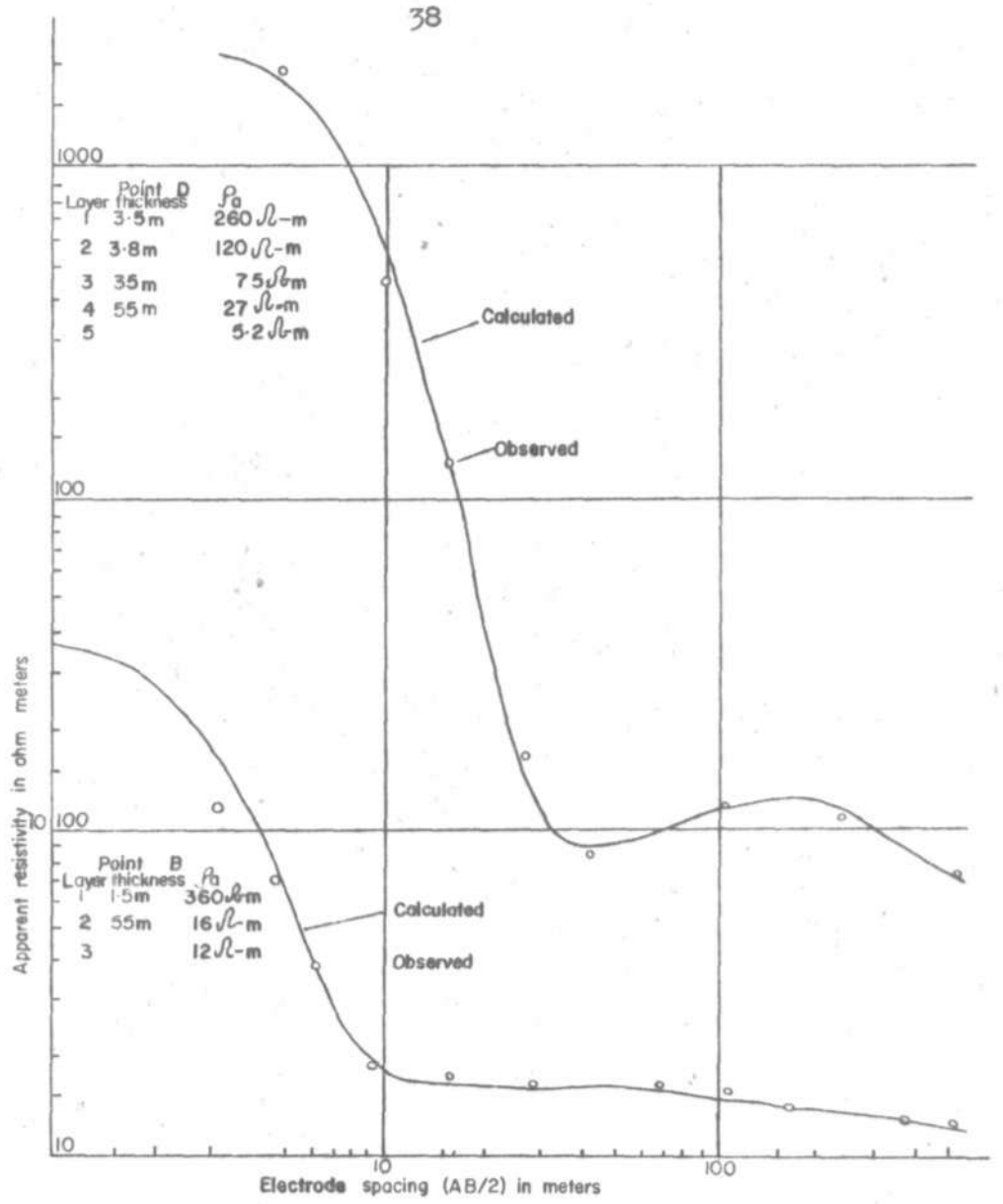



Fig. 4.3 a Interpretation of VES D and B curves

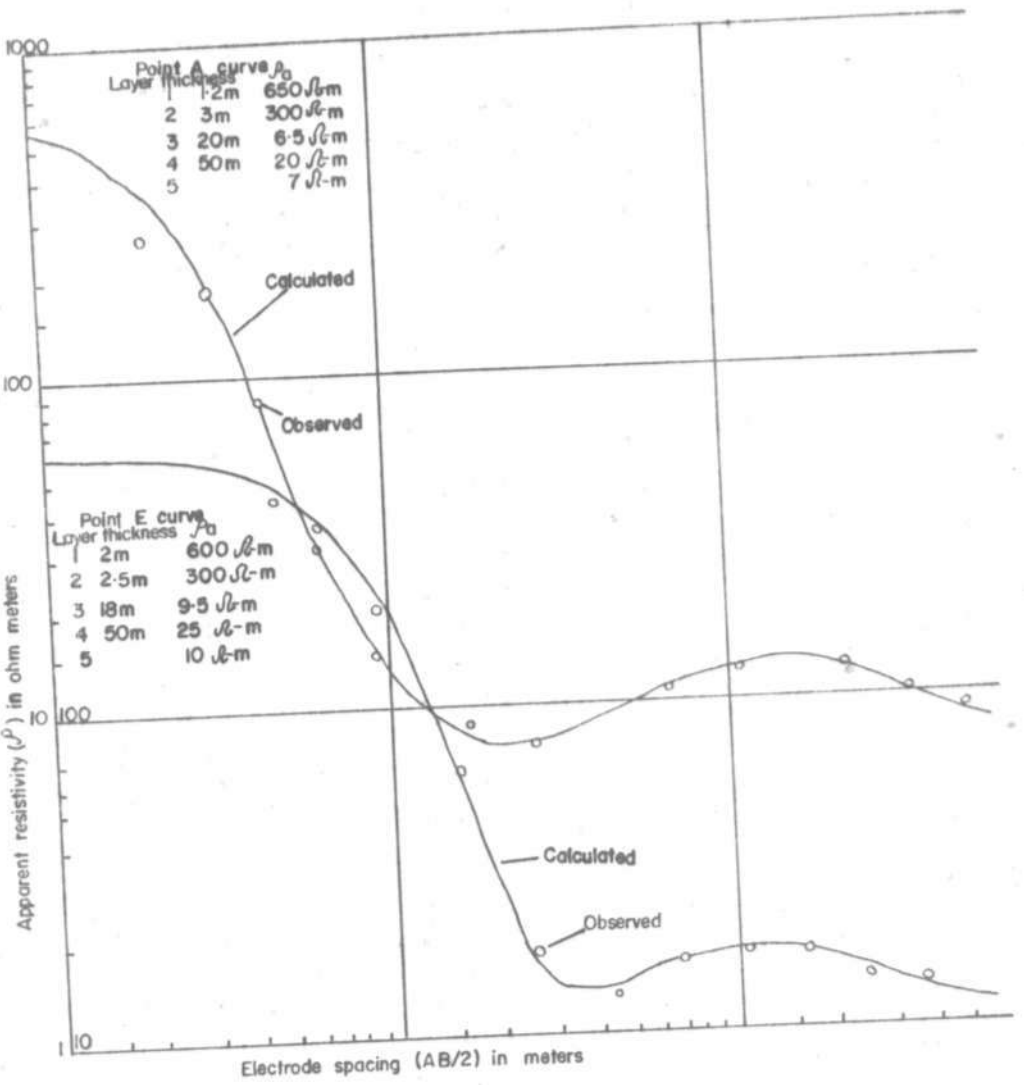
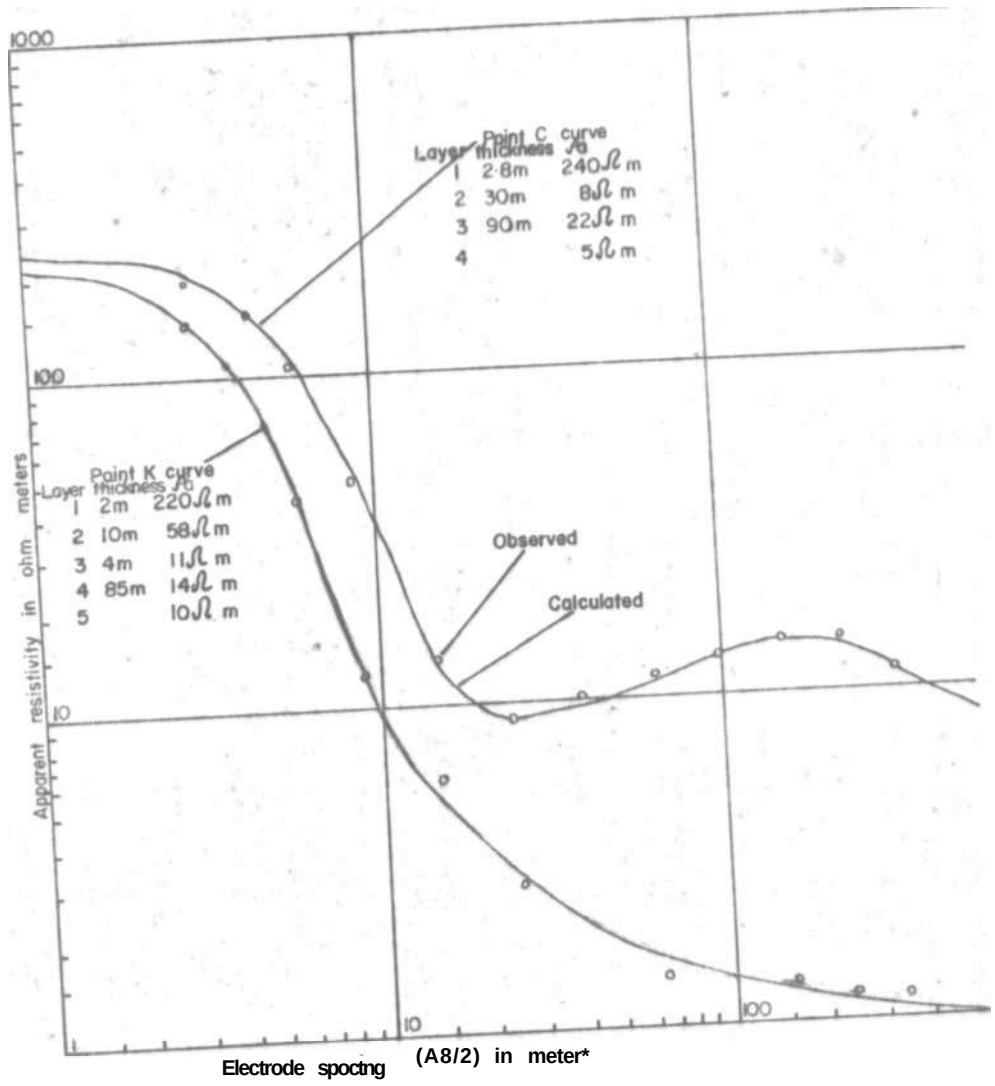



Fig. 4.3 b Interpretation of VES A and E curves




4.3 c Interpretation of VBS C and K curves

Table 4.1

Parameters obtained from Geoelectric Soundings

| Point | No of layers | Layer 1 | | Layer 2 | | Layer 3 | | Layer 4 | | Layer 5 | |
|---|---|---|---|---|---|---|---|---|---|---|---|
| | | Thick-ness $h_1$ m | Resis-tivity $\rho_1$ ohmm | $h_2$ | $\rho_2$ | $h_3$ | $\rho_3$ | $h_4$ | $\rho_4$ | | $\rho_5$ |
| A | 5 | 1.2 | 650.0 | 3.0 | 30.0 | 20.0 | 6.5 | 60.0 | 20.0 | | 7.0 |
| B | 3 | 1.5 | 360.0 | 55.0 | 16.0 | | 12.0 | | | | |
| C | 4 | 2.8 | 240.0 | 30.0 | 8.0 | 90.0 | 22.0 | | 5.0 | | |
| D | 5 | 3.5 | 2600.0 | 3.8 | 120.0 | 35.0 | 7.5 | 55.0 | 27.0 | | 5.2 |
| E | 5 | 2.8 | 600.0 | 2.5 | 300.0 | 18.0 | 9.5 | 50.0 | 25.0 | | 10.0 |
| F | 4 | 6.0 | 600.0 | 44.0 | 14.0 | 50.0 | 18.0 | | 9.5 | | |
| G top | 5 | 1.4 | 250.0 | 2.0 | 15.0 | 5.0 | 12.5 | 33.0 | 82.00 | | 38.0 |
| G lower | 2 | 30.0 | 20.0 | | 9.0 | | | | | | |
| H | 4 | 2.8 | 700.0 | 14.0 | 8.0 | 133.0 | 11.0 | | 9.0 | | |

Table 4.1 Contd.

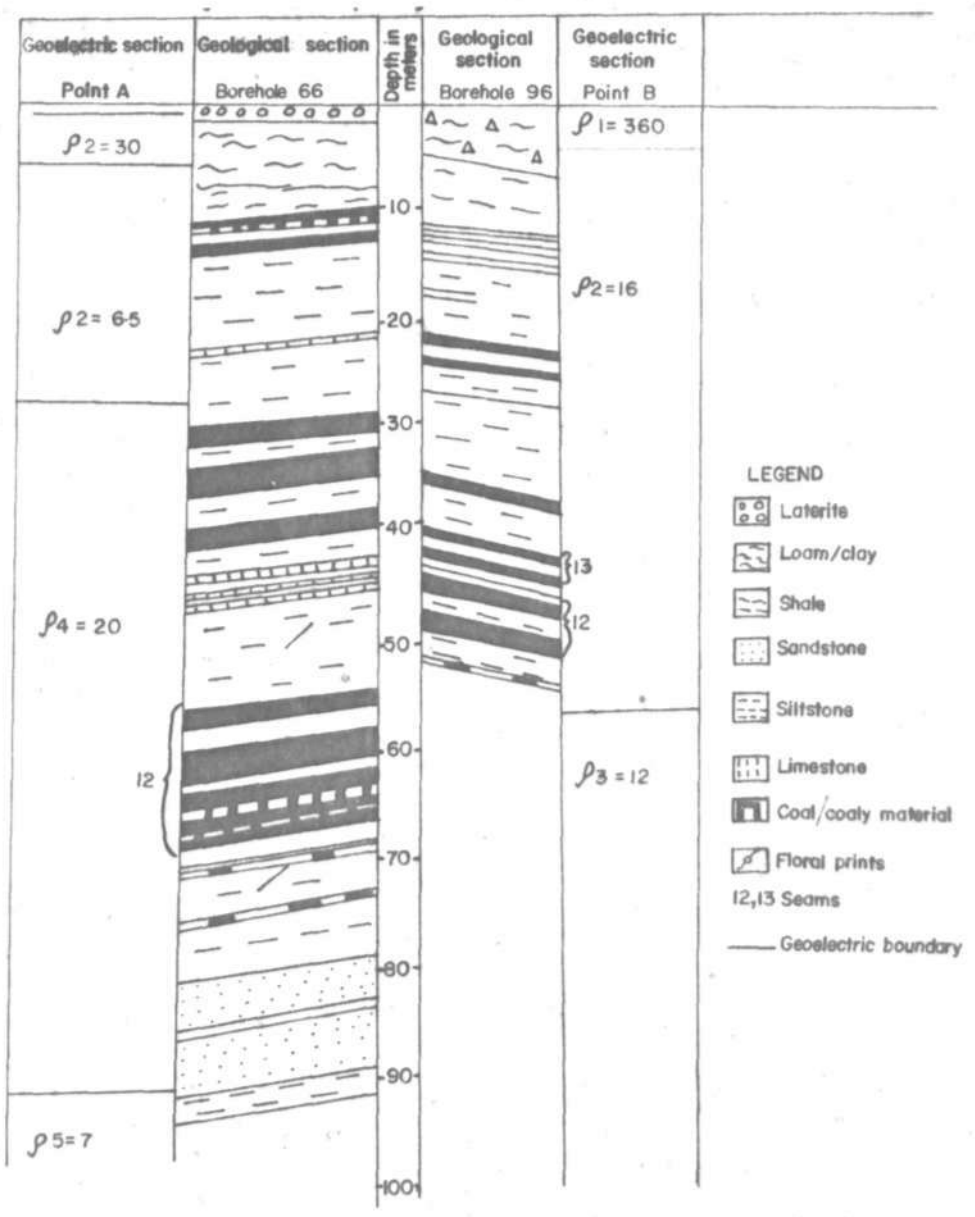
Parameters obtained from Geoelectric Soundings

| Point | No of layers | Layer 1 | | Layer 2 | | Layer 3 | | Layer 4 | | Layer 5 | |
|---|---|---|---|---|---|---|---|---|---|---|---|
| | | Thickness $h_1$ m m | $\rho_1$ ohm-m | $h_2$ | $\rho_2$ | $h_3$ | $\rho_3$ | $h_4$ | $\rho_4$ | | $\rho_5$ |
| I | 3 | 3.4 | 2400.0 | 9.0 | 55.0 | | 9.0 | | | | |
| J | 5 | 2.2 | 1000.0 | 3.0 | 30.0 | 17.0 | 8.0 | 50.0 | 15.0 | | 6.5 |
| K | 5 | 2.0 | 2200.0 | 10.0 | 55.0 | 4.0 | 9.0 | 85.0 | 14.0 | | 10.0 |
| L | 4 | 3.0 | 2500.0 | 6.0 | 120.0 | 10.0 | 22.0 | | 9.4 | | |
| N Top | 2 | 2.4 | 1100.0 | | 45.0 | | | | | | |
| N Mid | 3 | 7.0 | 100.0 | 60.0 | 8.0 | | 55.0 | | | | |
| N bottom | 2 | 80.0 | 20.0 | | 7.5 | | | | | | |
| R | 5 | 2.0 | 1400.0 | 5.5 | 93.0 | 20.0 | 17.6 | 62.0 | 32.0 | | 13.0 |
| S | 5 | 1.4 | 750.0 | 10.0 | 8.5 | 3.0 | 100.0 | 20.0 | 30.0 | | 6.0 |

host rock in the area which is shale. In general the ratio of the resistivity of the over-burden to that of the underlying structures is quite high, and of the order of 300:1 at some of the points. The data obtained for points A,B,D, and E, which are near boreholes 66,96,39, and 26, respectively were compared with the borehole geological sections Fig 4.4 (a,b). This helped to ascertain the exact electrical response of each rock type.

From the Fig 4.4 (a,b) it could be inferred that the overburden with high resistivity corresponds to laterite or laterite mixed with clay and sometimes includes loamy soil. The section with resistivity of 6.5 ohm-m to 10 ohm-m is likely to be mainly shale, the principal rock type. This shale may contain some amount of coal or carbonaceous material with the coal beds in this case, being very thin compared with the shale section. The section with resistivity from 10 ohm-m to nearly 30 ohm-m contains many coal seams situated at close intervals from one another, carbonaceous shale, sandstone and siltstone. The inter-bedding shale here is thin compared with the main shale zones.

The three main zones which have therefore been marked out are:-




4.4 a Comparison of Geological and geoelectric sections for points A and B

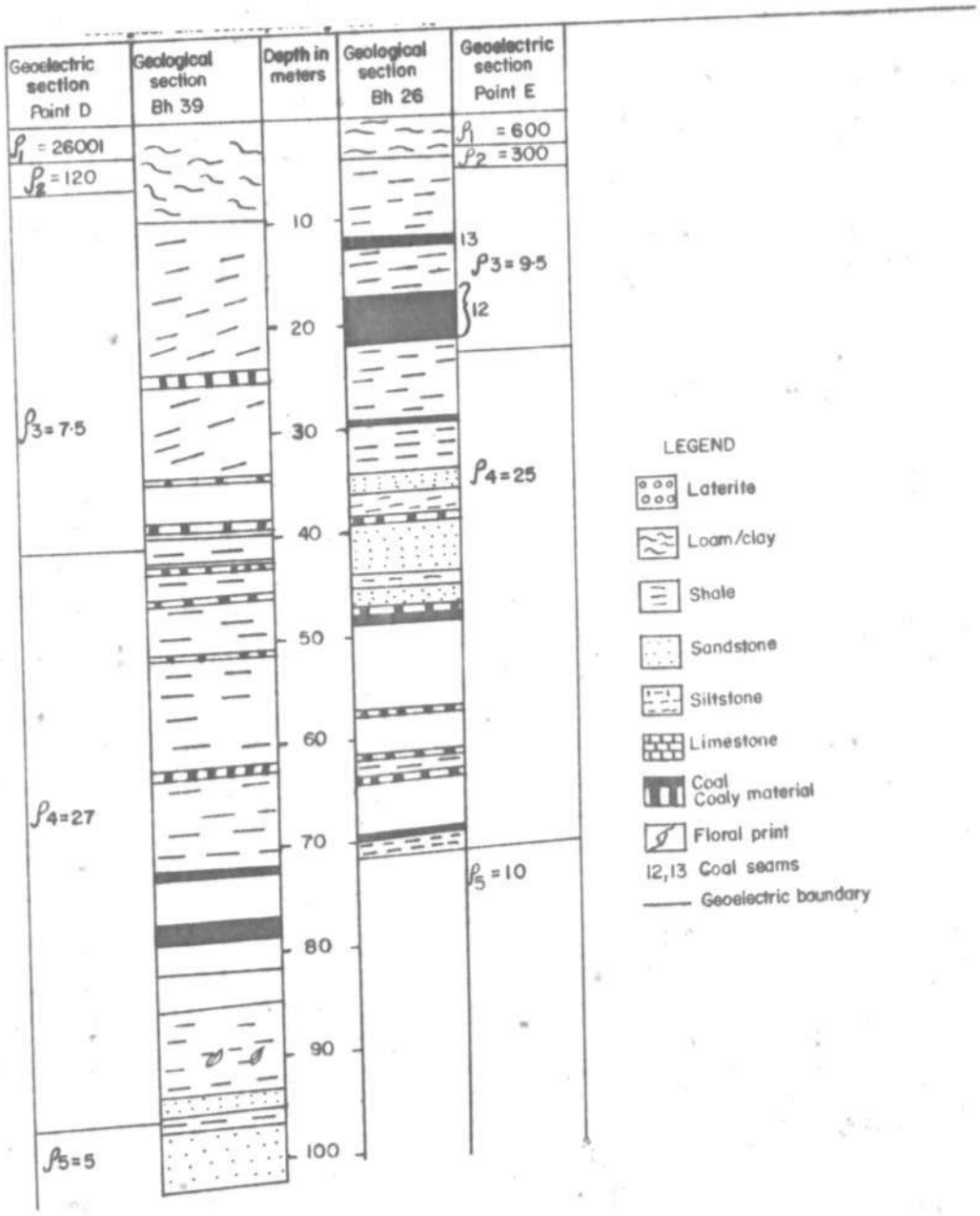



Fig. 4.4 b Comparison of geologival and geoelectric sections for points D and E

(i) a high resistivity over-burden (30 - 3000 ohm-m) consisting of laterite and clay.

(ii) a predominantly shally zone with resistivity from about 6.5 ohm-m to 10 ohm-m.

(iii) a zone consisting of an intercallation of coal, sandstone, shale, sometimes siltstone, limestone with resistivity from 10 ohm-m to 30 ohm-m.

At points G and N, geoelectric sections with resistivity as high as 55 ohm-m to 82 ohm-m were indicated at depth. The curves obtained at these points could not be matched by assuming any number of layer thicknesses and corresponding resistivity values. Rather, a combination of separate two-layer or three layer cases was used before obtaining good fits as shown in Fig 4.5. The lower section of the curves was of the K-type with very sharp curvatures unlike the usual gentle and broad peaked type encountered in other curves (E,D,A). These broad peaked curves were associated with mixed beds of shale, coal, limestone and sandstone. The sharp peaks exhibited by the curves for N and G suggest limited lateral extent (Zohdy et al, 1974) of these beds at a depth beyond 40 m in G and

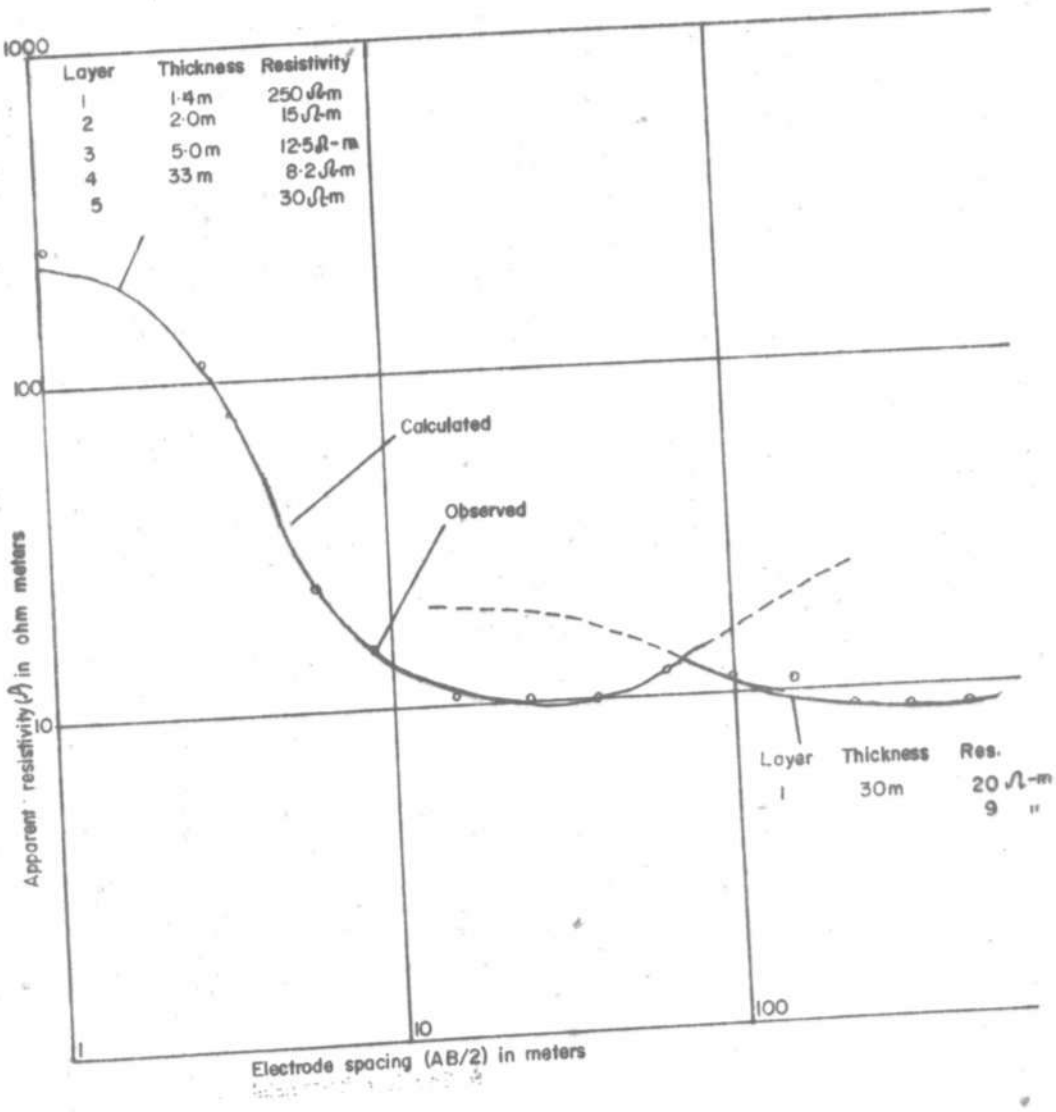



Fig. 4.5 Interpretation of VES G cuvre

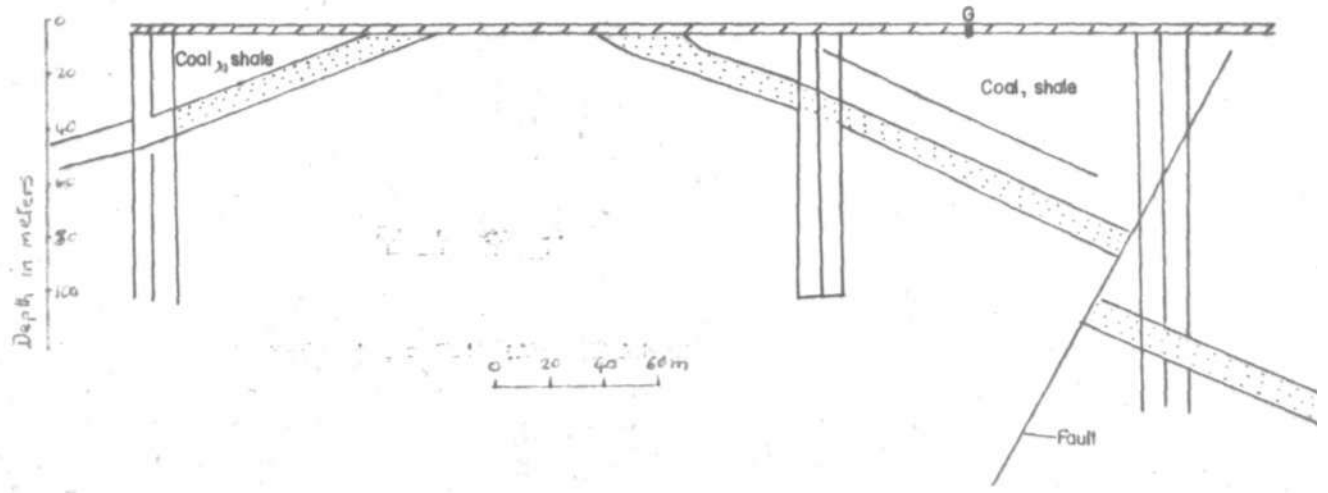



Fig. 4.6 Interpretation of VES G curve

70 m in N. A possible explanation is that the beds either thinned out or were faulted or there might exist a contact between formations with different resistivities. The geological section from a borehole just east of the point G revealed a fault (Fig 4.6) with approximate throw of about 55 metres. Such faulting might have taken place before the quarternary deposition took place which may explain why it is not apparent on the surface. In view of the above it may be assumed that the sharp peaks were due to faulting.

A geoelectric section for the points D,E and F is shown in Fig 4.7(a). This was constructed from the actual values of resistivities and thicknesses given in table 4.1 and by assuming that in between these points the geology is simple and the beds correspond to those derived from Fig 4.4 (a,b). A geological section linking the same points is shown in Fig 4.7(b).

A comparison of these two figures shows that there is some correlation between them. The shale zone with resistivity of under 10 ohm-m is well marked out from D to E but not beyond F. In the zone with resistivity above 14 ohm-m the boundaries do not correspond exactly. The arm XY

in Fig 4.7ais not shown in the geological section but is the first indication of perhaps the other flank of the anticline. This anticline is better shown by the geoelectric section along A B C Fig 4.7 c. The point C is far removed from B just as E is from D. Details of the geoelectric boundaries and hence geological boundaries may not be as simple as has been assumed. A better picture would have been obtained if more sounding points were located between D and E and between A and C.
Fig 4.7 d is the geoelectric section across K.E.L.

From these geoelectric sections it appears reasonable to redefine the resistivity limits as fixed earlier. The overburden resistivity appears to lie between 30 ohm-m to nearly 3000 ohm-m, the resistivity of shale appears to reach 14 ohm-m while the section containing inter-bedding of shale, sandstone, coal beds, and siltstone has resistivity from 15 ohm-m to nearly 30 ohm-m.

## 4.3 Resistivity Profiling

The profile layout is shown in Fig 4.1. In the field a qualitative observation of the sounding curves was made to determine which electrode spacings would give reasonable

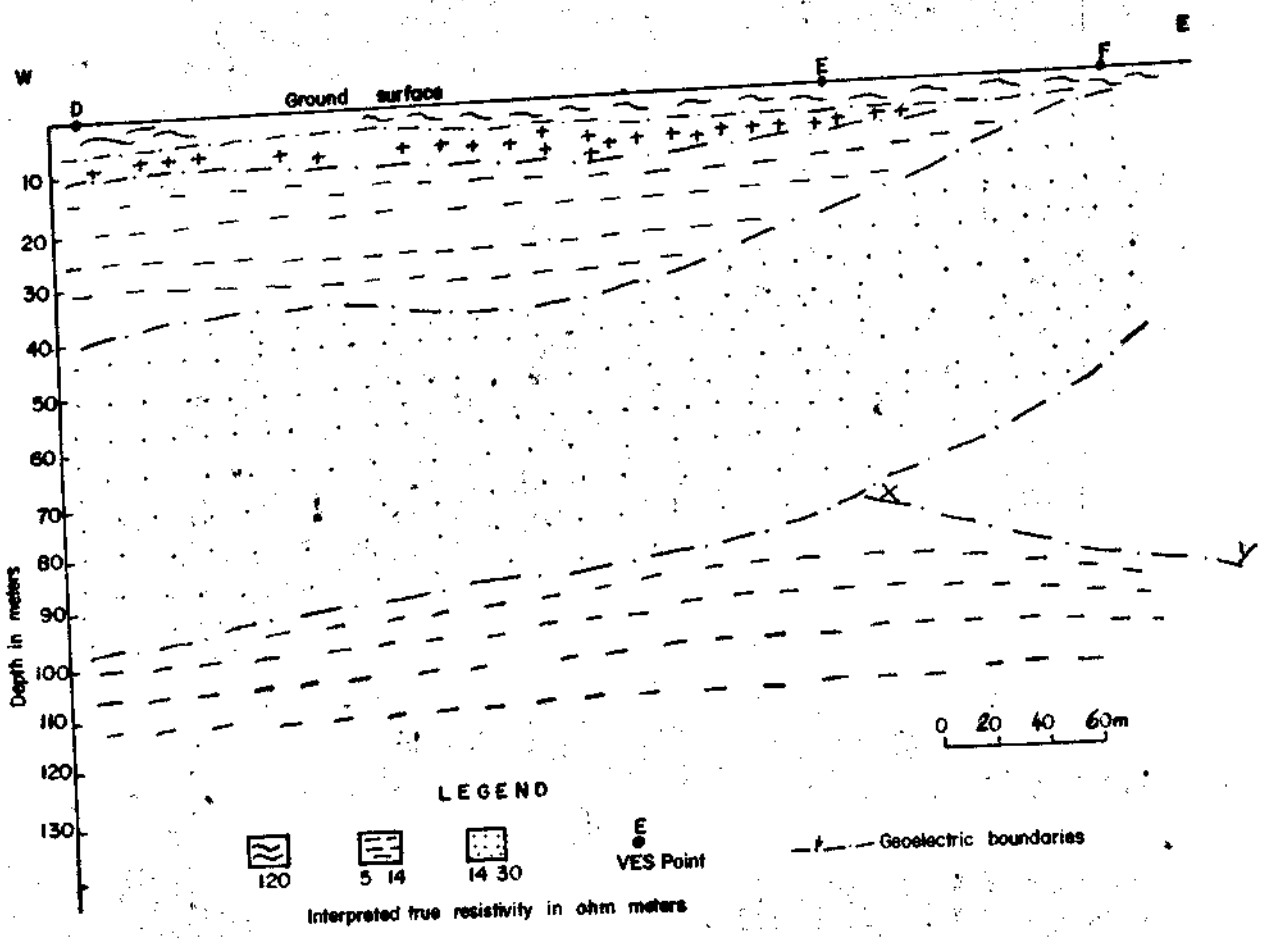
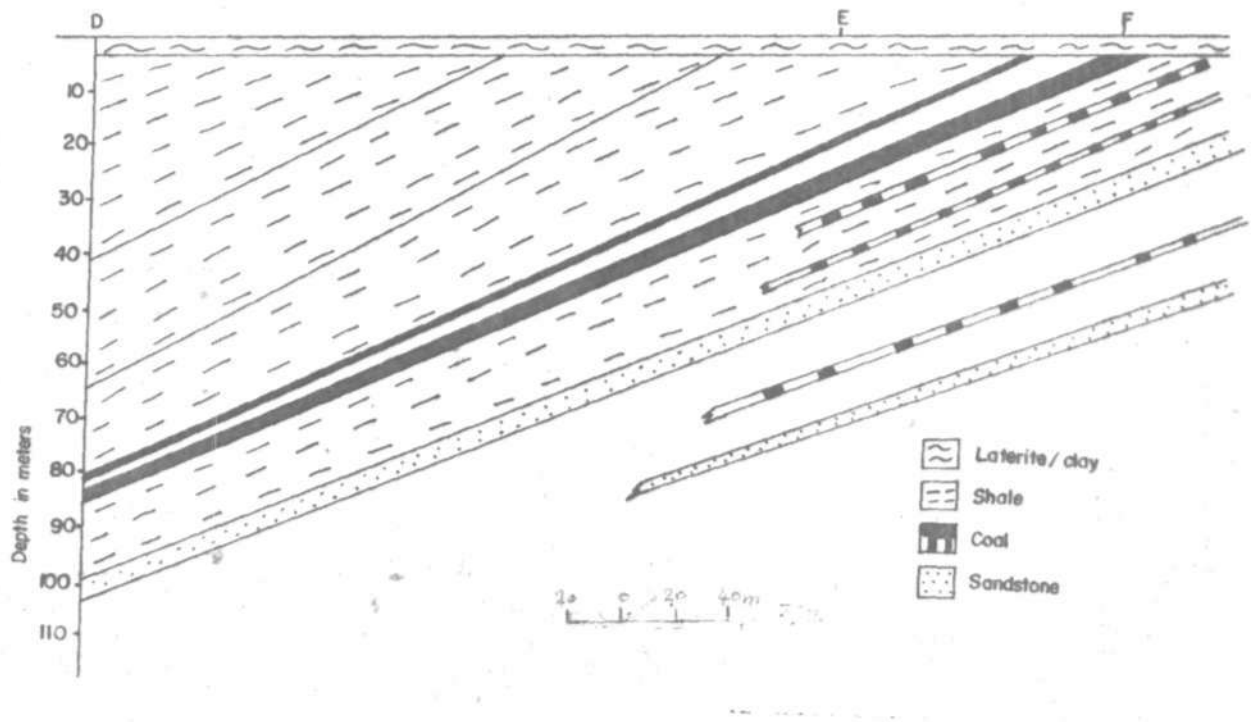



Fig. 4.7 a Geoelectric section along DEF




4.7 b Simplified geological section along DEF

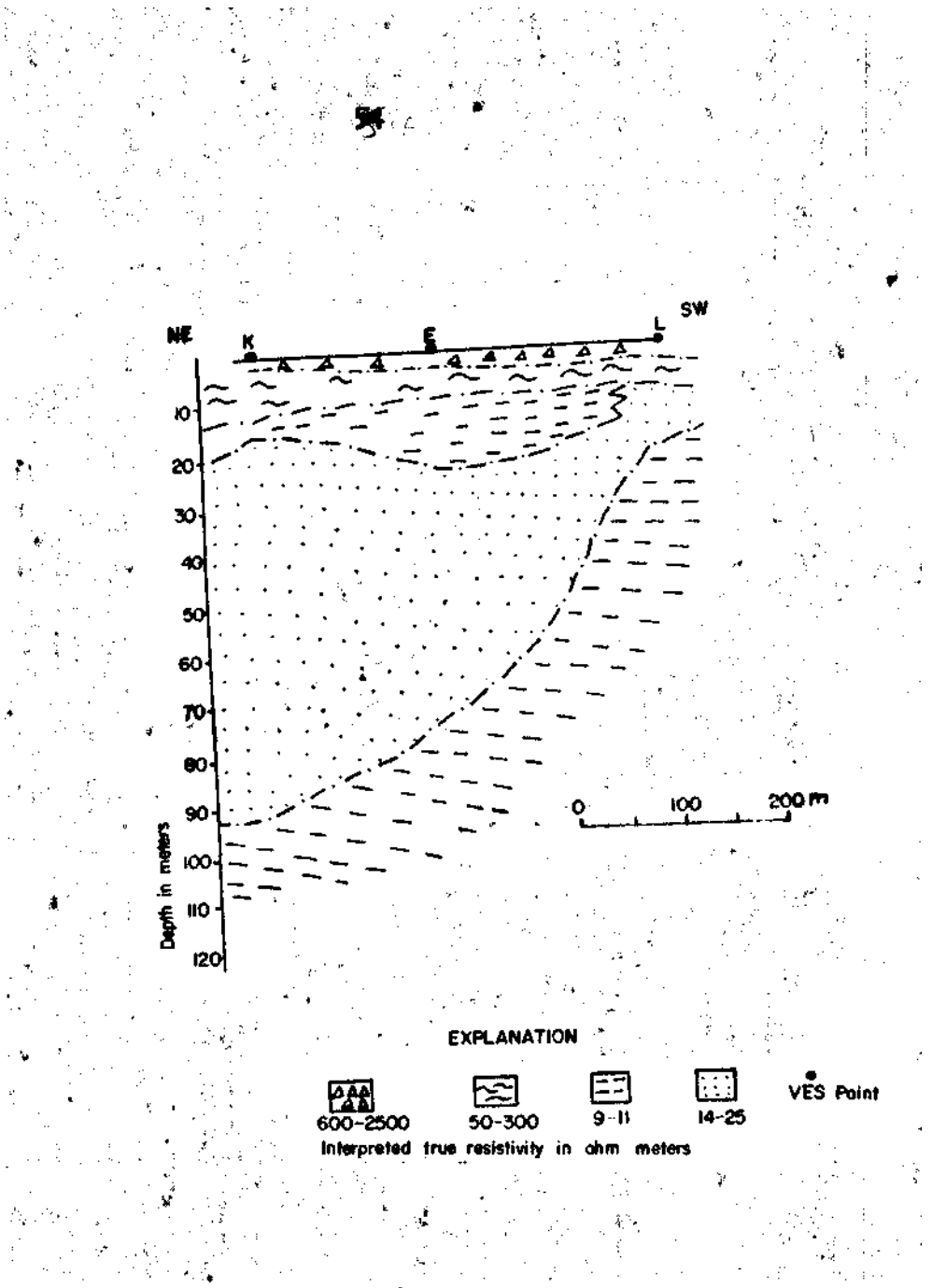



Fig. 4.7 d Geoelectric section across KEL

resistivity variations and hence different geologic sections. It was observed that total current electrode spacings of 75 m, 150 m, 225 m generally corresponded to three resistivity zones. On this basis, it was decided to do profiling using Wenner electrode configuration with constant electrode separations of 25 m, 50 m, 75 m corresponding to the above current spreads.

Resistivity profiling was then carried out along profile 1 using the three electrode spacings mentioned above. Apparent resistivities were determined at each station from values of V and I according to the formula

$$\rho = \frac{2\Pi\, b\, V}{I} \qquad \text{(Parasnis, 1975)}$$

where b is the electrode separation, V the measured voltage in mV and I the measured current in mA. The apparent resistivities along the profile were then plotted for each of the three electrode spacings. Inspection of these plots showed that the 25 m and 75 m separations gave better indications of the lateral variations in resistivity. Three more profiles II, V and VII were therefore surveyed using these two spacings and the results plotted for each

of the spacings Fig 4.8, 4.9. Contour maps of the results were prepared with a contour interval of 5 ohm-m (Fig 4.10, 4.11). From these contour maps it was realised that 25 m electrode spacing gave still better picture of the variations and two more profiles IV and VI were surveyed using this spacing to complete the contours of Fig 10.

A close study of Fig 4.8 reveals that along each of profiles IV, V and VI resistivity highs reaching up to 40 ohm-m occur to the north of these profiles. Resistivity highs also occur along the middle part of profiles II and IV. On all profiles the resistivity values generally show higher values to the northern half than to the south. The values to the south rarely exceed 10 ohm-m but are higher than 15 ohm-m northwards.

The contour map Fig 4.10 shows two anomalous zones, one to the north and the other in the middle of the survey area. The anomaly to the north suggest a geological structure trending approximately east-west. The boundary of this anomaly could be a fault, an ordinary contact or possibly a folding. In order to investigate this boundary, points S,R,W, and T were selected for sounding. The electrode spread was then oriented in the East-West

direction as against NE-SW for the other points. The soundings at W and T gave very irregular curves inspite of repeated readings and therefore could not be interpreted. Points R and S, however gave normal curves the sections of which are given in table 4.1.

From the geoelectric sections at R and S it is easy to conclude that a kind of transition zone exists between them. The sections strongly suggest a contact. At R the general abscence of a shale zone ($\rho_a$=5 ohm-m - 14 ohm-m) is remarkable for the first 50 m or more. The resistivity of 17 ohm-m to 30 ohm-m suggest a thick zone of interbedding of moderately high resistive rock types like sandstone with possibly high content of carbonaceous material and limestone. At S a 10 m shale bed underlies the overburden, and a section with rather high resistivity but thin (thickness 3 m) follows. The section with 3 ohm-m resistivity is an indication of a good conductor. Some aquifer can thus be inferred.

The sections at R and S are thus not easily correlated and a transition zone is definitely established.

The resistivity high around the centre of Fig 4.8 was thought to be due to the effect of the laterite apparent on the surface in this area but the steep contours across UV give positive indications of some kind of contact.

4.4 Limitations and error in the Resistivity Work

A survey of the type described above contains certain sources of error. The most fundamental is error arising from the caliberation of the meter. In section 3.1 it has been stated that the error on the voltage and current measurements was not more than 2%. Thus the maximum error expected in the resistivity measurements would not exceed 4%.

Most of the curves depict multi-layer geologic structure. The curves were mostly K-, H- and KH-types. Generally the interpretation of such curves is not unique (Zohdy et al, 1974). This means that a given electrical sounding curve can correspond to a variety of sub-surface distributions of layer thicknesses and resistivities. The principle of equivalence also contributes to the error in conventional methods of electrical soundings.

IBRAHIM LIBR

The quantitative contribution cannot be easily assessed. Added to this is the obvious occurence of suppression. In curves where the resistivity of the surface layer decreases monotonically (point B) it is noticed that the curves resemble a two-layer earth model which will no doubt obscure the detection of the coal beds particularly in view of the fact that their relative thicknesses are small.

# CHAPTER V

## SELF-POTENTIAL(SP) METHOD

### 5.1 The Origin of Self-Potential

Whenever two non-polarizable electrodes are driven into the ground and connected to the terminals of a sensitive voltmeter, an electric voltage is found to exist between them. The voltage so measured is of the order of millivolts. The potential differences between two points are partly constant and partly varying with time. They are associated with the flow of electric current in the host rock. Above sulphide bodies for example pyrite, chalcopyrite, pyrrhotite and graphite bodies they may attain values of several hundred millivolts to 1 volt (Dobrin,1976; Parasnis,1975). Large voltages have also been reported over anthracite coal (Parasnis,1975).

The potentials are usually set up as a result of electro-chemical actions in the rocks' interfaces or in bodies embedded in them. Self-potentials observed on the ground can be broadly divided into two classes namely:-

(i) the small 'background potentials' ranging from a fraction of a millivolt to a few or few tens of millivolt, and

(ii) the mineralization potentials with maximum values of the order of a few hundred to several hundred millivolts. The background potentials can have varying polarity whereas the mineralization potentials are in general negative (Parasnis, 1975) - Some of the background self-potentials are due to the variations in the concentration of the electrolytes in the ground including groundwater with dissolved salts. Some others are caused by steaming water through the pores of rocks, which create capillary effect with potential gradient between the ends of the capillary.

Mineralization potential is explained by the existence of potential difference between the oxidized top and lower ends of an ore-body (Parasnis, 1975). This, however, is not true of some minerals for example graphite which produces self potential without undergoing any oxidation. In the Obi coalfield, traces of pyrites have been discovered amidst

shale core samples. The water table in the area is not clearly mapped but is supposed to exist before the coal beds. Such water is unlikely to be free of pollution by dissolved pyrites and other salt solution within the shale. A self-potential measurable in the area is therefore likely to be caused by either the background or mineralization or even a combination of both especially as water with high salt content is forced into fault zones.

5.2 Field Procedure and Data Reduction

Measurements were made along profile V which was also one of the gravity and resistivity profiles. The equipment comprised two non-polarizable electrodes each consisting of a copper rod placed in a porous pot containing saturated copper sulphate (Cu $SO_4$) solution, cable reel and a voltmeter that read to an accuracy of 0.2 millivolts. The range of calibration of the meter was between 0.2 to 1000 millivolts. The meter is of the null type and reading at each station was obtained by adjusting the needle until it rested on the null line when contact with the ground was assured through the porous pots.

The method adopted was the potential method. In this, one of the electrodes was buried permanently at the point M (Fig 4.1) regarded as the base station. The second electrode, together with the cable reels and the voltmeter were advanced to different stations as the cable was laid off. The electric potential of each point was thus read on the meter relative to that of M. The stations were located at 25 meters interval.

The readings obtained were first corrected for elevation effect. Elevation changes invariably affect the self-potential measurable in an area because they cause voltages in the earth which may not be easy to predict (Dobrin, 1976). In the portion of the field data free from disturbances it was noticed that a near linear relationship existed between the change in elevation and the change in self-potential between stations. Fitting a straight line to the data by means of a least square method, a gradient of 3 $mV/m^{-1}$... was obtained. The equation of the fit is of the form:

$$\Delta SP = -3\Delta H - 23$$

where $\Delta$ SP is change in self potential, $\Delta$H is the

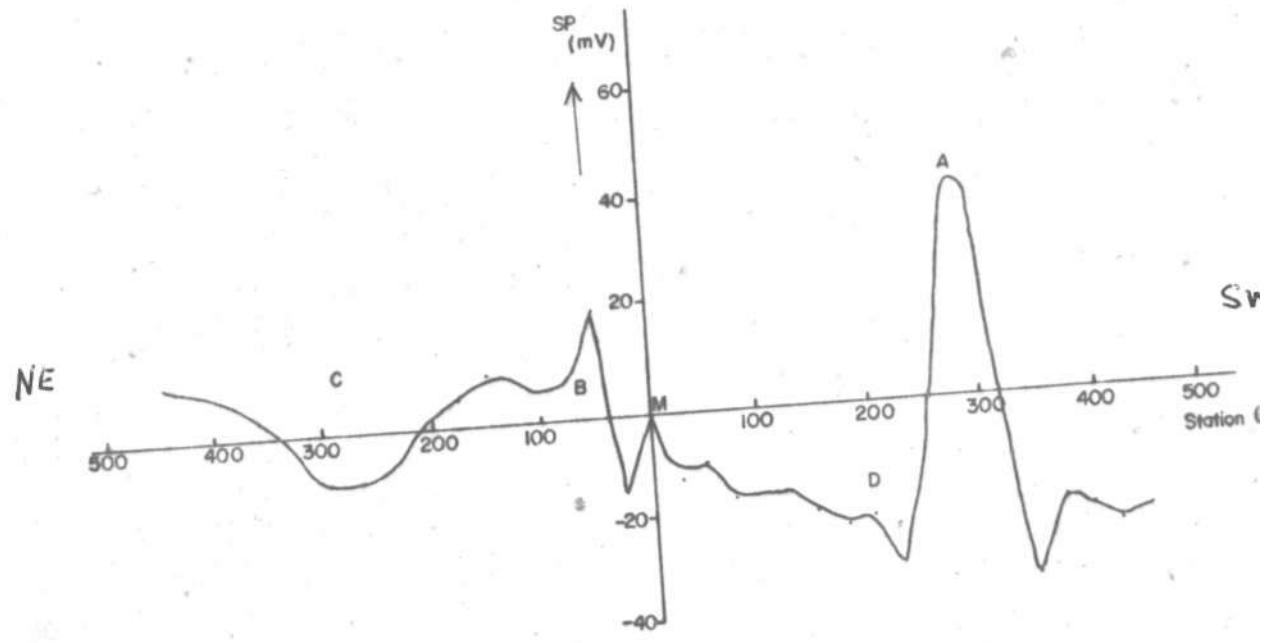



Fig. 5.1 Plot of SP values corrected for topography

corresponding change in elevation. The constant (-23) contains the regional effect and is likely to vary over a large area. The elevation correction was added to all the values and the reduced data are shown in Fig 5.1.

## 5.3 Description and Interpretation of SP Anomalies

A close look at (Fig 5.1) reveals two obvious anomalous zones 'A' and 'C'. 'B' appears to be the effect of some unpredictable spurious source and is not considered. 'A' occurs S.W. of the profile reaching a sharp maximum of over 30 mV above the downward trend. It is most likely a response to a near surface source. The change from the normal regional value (about -23 mV) is sudden and the fall back is even more precipitious. The positive high here has removed the possibility of an orebody which has generally a negatively high self-potential (Parasnis, 1975) but positive potentials are the results of the chemical activity in the earth and can therefore be of other geologic origin. It is to be noted that A attains its peak value at a point which corresponds to a maximum value of the elevation but the anomaly is too big to be considered a topographic effect outright.

N.E. of the profile occurs another broader anomaly 'C' with a negative low of about -10 mV. The broad nature and magnitude of this anomaly suggest a deep-seated structure. The negative low here is not low enough to suggest mineralization straight away. One can therefore, attribute the anomaly also to some other geological feature. Since the elevation in the area is uniform, the topographic effect is likely to be negligible too.

In order to interprete the data quantitatively, a theoretical body whose SP effect on the surface would fit the observed was sought. The potential due to a line charge at any point r, outside its axis is given by:

$$V(r) = \frac{K\lambda}{4\Pi\varepsilon_o} \ln r \qquad \ldots.(1)$$

where $\lambda$ is the current density, $\varepsilon_o$ is the permittivity in vacuum and K is a constant, (Sears et al,1970). For two line currents with opposite charges the potential at any point distant $r_1$ and $r_2$ from the lines is given by

$$V = C \ln \left(\frac{r_1}{r_2}\right) \qquad \ldots.(2)$$

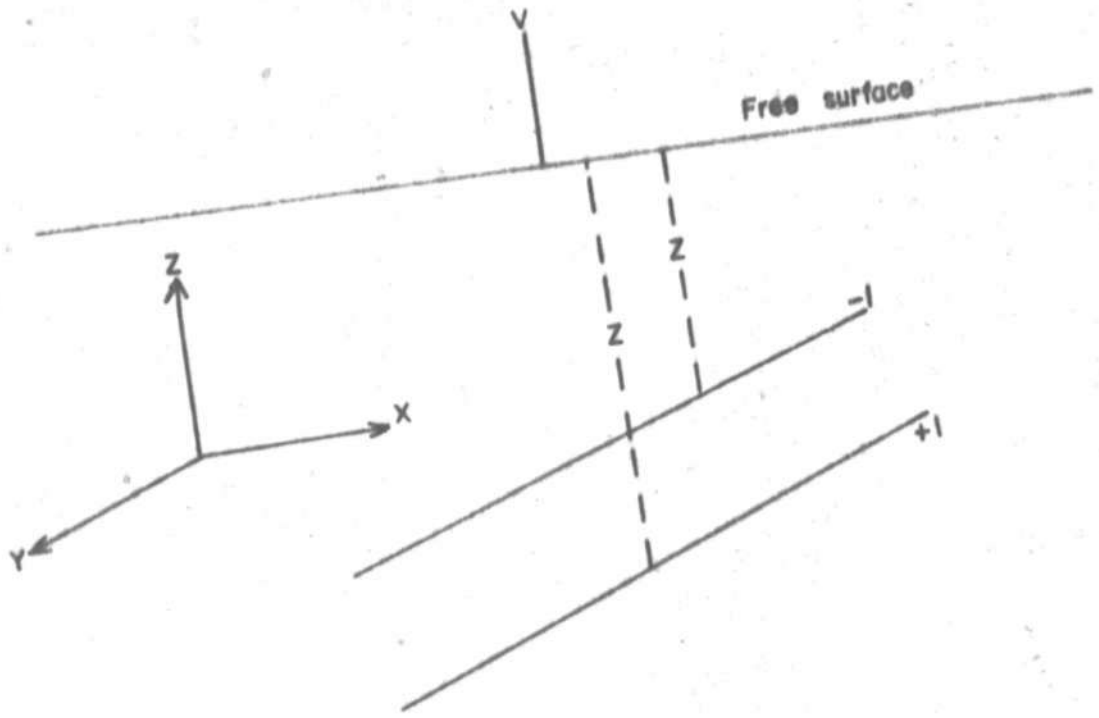



Fig. 5.2 A sketch of the line likely to give rise to an SP anomaly.

where C is a constant.

If we then imagine a vertical structure within the earth whose upper and lower boundaries are represented by two line poles with linear current densities -I and +I respectively and extending theoretically from $-\infty$ to $+\infty$ in the direction parallel to the y-axis and cutting the x -z plane at points $(x_1, z_1)$ and $(x_2, z_2)$ (Fig 5.2), then the potential due to this pair of lines at any point on the surface is given by

$$V(x) = C \ln \left( \left[ (x - x_1)^2 + z_1^2 \right] / \left[ (x - x_2)^2 + z_2^2 \right] \right) \quad \ldots(3)$$

Here C is a constant depending on the resistivity of the surrounding rock and its unit is mV. The symmetry nature of the anomalies suggest vertical structures, as reasonable models.

In order to determine the parameters in equation (3) which would provide the SP effect sought, a computer programme employing the theory of non linear least squares method and designed for use in the department of

Physics mini-computer (Verheijen, "personal communication") was used. Test values of the coordinates of the line charges, the constant C and another parameter representing any regional effect were introduced into the programme. The computer calculated the SP effect from these test values, and then compared the calculated and the observed. Then it continued to adjust the parameters by a non-linear least squares process, computing new parameters until the sum of the squares of the errors between the observed and the calculated anomalies was minimized.

Fig 5.3 a,b, show the combined plot of the observed and the calculated with the positions of the line charges which point into the paper. The fit for anomaly C is good with a standard deviation of 1.82 mV. The fit for anomaly A is not very good especially around the edges of the anomaly. The error here is of the order of 2.2 mV. The bad fit here might have arisen from the fact that the orientation of the line charges is not strictly correct or that measurements were wrong.

Fig 5.3a shows that the anions are concentrated nearer the surface than cations and the general orientation of the line charges suggest a near vertical geological

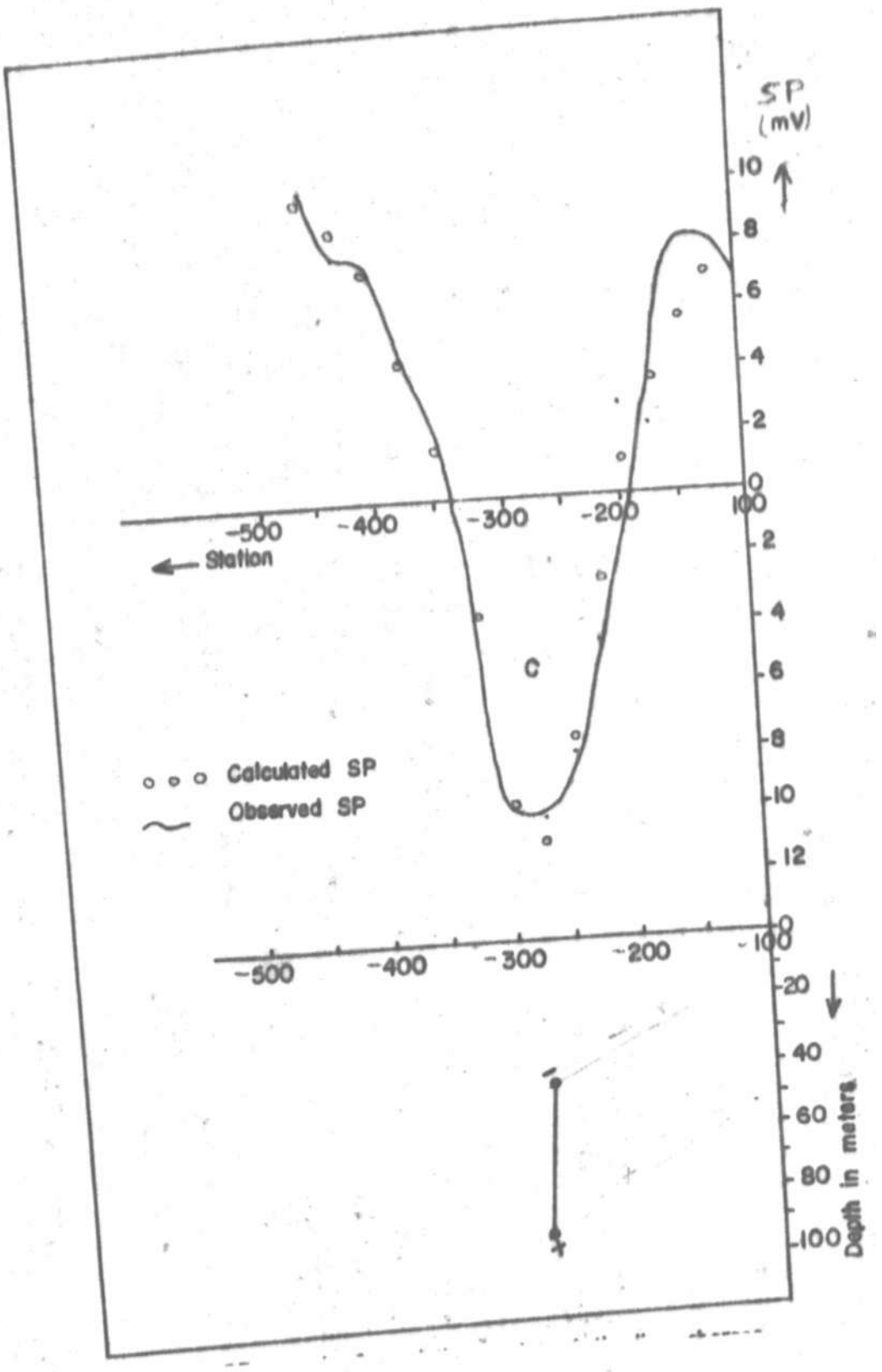



Fig. 5.3 a SP anomaly 'C' and the model of the line charges

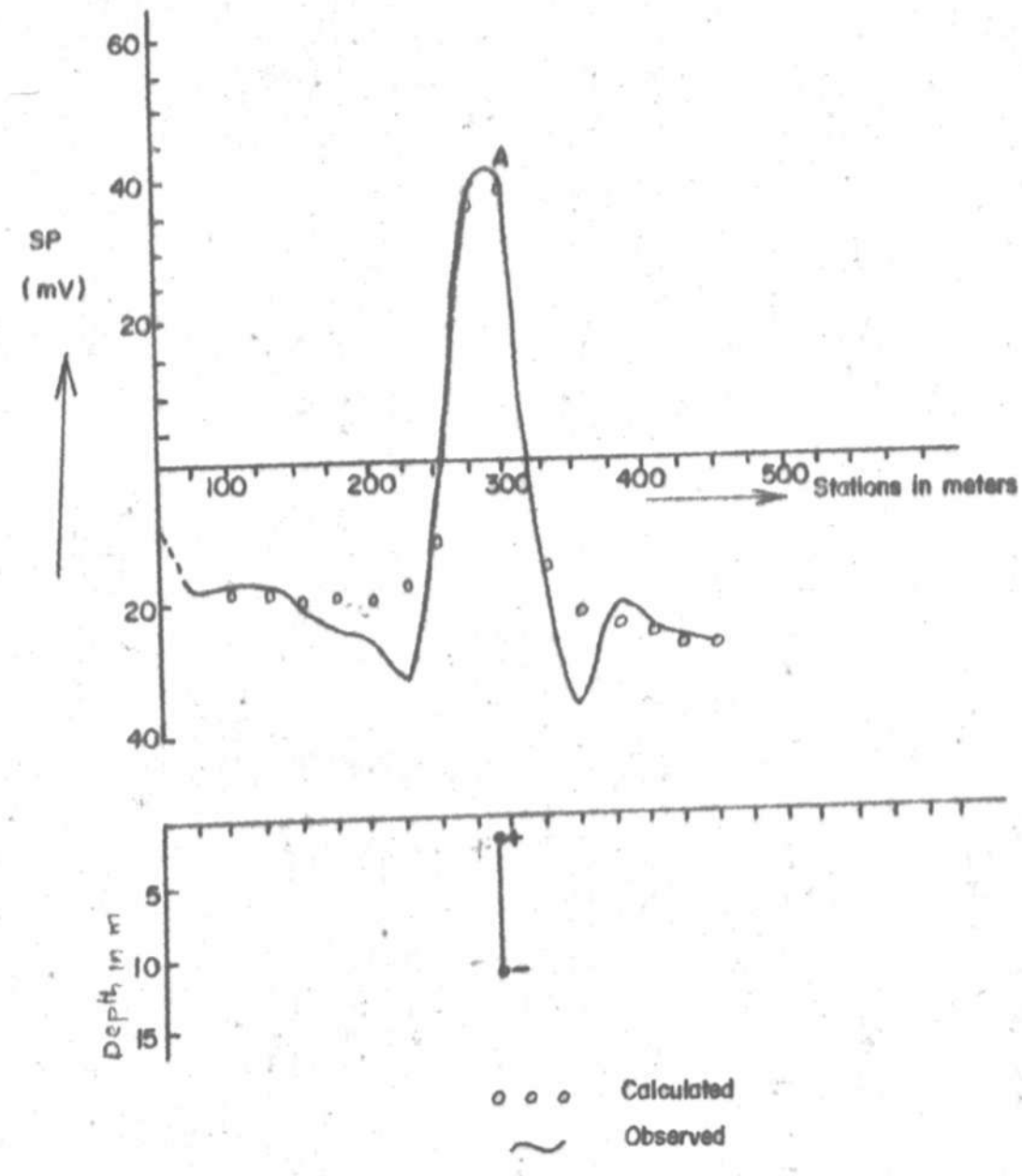



Fig. 5.3 b SP anomaly 'A' and the model of line charges

structure enlongated in the direction perpendicular to that of the profile, that is near E-W. The structure is assumed to have a reasonable concentration of some electrolyte which favour the movement of ions giving rise to the self-potential observable at the surface. Geological information (Okeudo, 'personal communication') shows that fault zones in Obi area are associated with impregnation of calcite. This might have resulted from the evaporation of $CaHCO_3$ (Calcium bi-carbonate) which infiltrated into the zone after faulting. $CaHCO_3$ itself being a weak electrolyte can favour electrolytic action giving rise to the self-potential which has been observed. It is reasonable therefore to associate this anomaly at C with a fault or contact trending E-W in agreement with the orientation of the line charges.

The model for anomaly A suggests a pair of line charges also oriented in the E-W direct. One may again attribute this to a fault zone but during the modelling the depth to the +ve line could be varied between 1 m to 3 m below the surface without appreciably affecting the fit. This means that the +ve line charge lies within

the overburden and if it represents a fault, this should be observable at the surface, but this is not so. It is therefore more likely that this is an ordinary surface effect which can be attributed to the turning point in elevation near the anomaly.

# CHAPTER VI

## GRAVITY METHOD

### 6.1 Field Work

Gravity readings were taken along two parallel profiles II and V and a cross profile VIII (Fig 4.1). The point E was chosen as the base station and all other measurements were made relative to it. The instrument used was a C-G2 gravitmeter belonging to N.S.D.A., with a reading accuracy of 0.01 mgal and instrument constant of 0.09668 mgal/division. Since this gravimeter was not available when the survey was being planned, it was not possible to observe its behaviour with respect to drift before the survey. However repeat observations were made at the base station at intervals not exceeding 2 hours.

The elevation of each station was determined relative to the base station by means of a spirit level. All levelling began and ended at point E and the closure error for all the measurements never exceeded 0.2 meter. The maximum error in the Bouguer anomalies due to inaccurate elevation determination would therefore not

exceed 0.06 mgal.

6.2 Density Determination

Borehole core samples of the representative rock types in Obi area were collected for density measurements. These included samples of clay, shale, sandstone, sandstone/siltstone and limestone. It was however, not possible to obtain coal samples from core because all coal samples had been removed by field geologists. The samples used were taken from those mined from a test shaft.

The dry bulk density and the saturated bulk density of the samples were calculated whenever possible. The samples were first weighed in air $(W_A)$ then in water $(W_w)$. They were completely submerged in water for 24 hrs. They were then weighed again in air $(W_{dA})$ and in water $(W_{dw})$. The dry density was calculated using the formula

$$S = \frac{W_A}{W_{dA}-W_{dw}} \quad \ldots.(1)$$

Where it is not possible to measure $W_{dA}$ the dry density was obtained from

$$S = \frac{W_A}{W_A-W_w} \quad \ldots.(2)$$

The bulk saturated density $S_d$ was calculated using the formula

$$S_d = \frac{W_{dA}}{W_{dA}-W_{dw}}$$

In most cases it was not possible to measure the saturated density due to the disintegration of samples when submerged in water for a long time. In other cases the samples' surfaces were so baked that submerging them made no difference to the measured densities. Hence it was found necessary to use only the dry bulk densities. A summary of the mean densities with their standard deviations is give in Table 6.1.

Comparing the values with those of some other workers in the area showed that the density determined for shale was low. The Nigerian Steel Development Authority (Migraev, "personal communication") obtained a dry density of $2.5 \times 10^3$ kg/m$^3$. A density of $(2.50 - 2.55) \times 10^3$ kg/m$^3$ was accepted for modelling purposes in the area by Cratchley and Jones (1963). The low value of $2.45 \times 10^3$ kg/m$^3$ obtained in this work might be due to the fact that most of the samples used in the density determinations were weathered. In view of this a dry density value of $2.5 \times 10^3$ kg/m$^3$ for

shale was assumed in the analysis of gravity data.

Table 6.1

Densities of Different rock types in Obi Coal Deposit

| Rock type | No of Samples | Range of Densities x $10^3$ kg/$m^3$ | Mean & Std. Dev. x $10^3$ kg/$m^3$ |
|---|---|---|---|
| Sandstone | 16 | 2.28 - 2.65 | 2.45 ± 0.01 |
| Siltstone/ Sandstone | 6 | 2.14 - 2.57 | 2.45 ± 0.01 |
| Shale | 18 | 2.33 - 2.69 | 2.45 ± 0.02 |
| Coal | 8 | 1.49 - 1.79 | 1.68 ± .03 |
| Clay | 4 | 1.99 - 2.03 | 2.01 ± 0.00 |
| Limestone | 3 | 2.66 - 2.8 | 2.73 ± 0.00 |

## 6.3 Reduction of Data

All the gravity data were reduced to Bouguer anomaly values using the standard reduction formulae (Dobrin, 1976; Parasnis, 1975) and were relative to the base station. The relevant corrections applied are:

(a) Drift Correction In calculating the drift for each station a linear relationship between gravimeter readings and time was assumed. The time interval for reoccupation of the base station was less than two hours. The drift rate is then given by

$$\delta = \frac{R_2 - R_1}{t_2 - t_1} \qquad \ldots(1)$$

where $R_1$, $R_2$ are the readings at the base station at the times $t_1$ and $t_2$ respectively.

The observed reading corrected for drift for a station is given by

$$\Delta g_d = K(R_3 - R_1) - \delta(t_3 - t_1) \ldots(2)$$

where $R_3$ is the reading in scale units at the station at time $t_3$ and K is the instrument constant, $R_1$ the reading at the base station.

(b) Latitude Correction In each hemisphere the gravity increases towards the respective pole giving rise to a normal gravity difference between a station and a base station due to the latitude difference between them. Since in the area of survey the distance between the base station to any station was less than 2 km the latitude correction is given by

( $\Delta g$ = 0.00081 sin 2$\phi$ mgal/m north-south distance) where $\phi$ is the latitude of the base station. This correction was added for stations south of the base station and subtracted for those stations north of the base station (Parasnis, 1975; Grant & West, 1965).

(c) Free air or elevation correction The earth's gravitational force decreases with an increase in elevation above the surface of the earth giving rise to a vertical gravity gradient. The Free-air correction to be applied to all gravity readings is generally given by

$$\Delta g_{FA} = \frac{dg}{dz} h$$

where $\frac{dg}{dz}$ is the vertical gravity gradient and h is the height of the station relative to the base. This is equivalent to 0.03086 h mgal where h is in meters and is added if the station is higher up than the base, and subtracted from it if it is lower down. (Parasnis, 1975; Dobrin, 1976).

(d) Bouguer Correction The free-air correction discussed above has taken into consideration only the fact that the base station and the station of observation are not at the same distance from sea level. The Bouguer correction accounts for the attraction of the rock material between the base and the station at elevation h. The material is approximated to an infinite horizontal slab of thickness h and density $S$ and the gravitational attraction of such a slab is $0.04191S$ mgal per meter. This value is subtracted from the measured gravity difference if the station is above the level of the base station and added if the station is below the base station.

After all the corrections were determined as described above the Bouguer anomaly was obtained using the formula

$$\Delta g_B = \Delta g_d \pm \Delta g_\phi + (0.3086 - 0.04191S)h \text{ mgals}$$

for h positive with respect to the base station. Since the terrain in the area is relatively flat, the highest elevation difference encountered was only 12 m, the

This will introduce an error of about 2 x 2 x 0.00081 sin ($17^{o}$ 14') or 0.001 mgal which is insignificant.

If the maximum possible error was made in all determinations at any one station, then the maximum Bouguer anomaly error for the station would not exceed 0.06 mgal.

6.5 Description and Interpretation of Bouguer anomalies

The Bouguer anomaly values were plotted for the three profiles as shown in Fig 6.1 (a,b,c,). All have one feature in common, that is the variation in the Bouguer anomalies is generally low. The highest value above the base station value is not more than 0.6 mgal along profile V and 0.3 mgal along profile II. The small variation in the anomalies suggest that measurements were taken over a fairly geologically homogeneous region. This agrees with the work of Cratchley and Jones (1963) in which Obi falls within a region with gentle Bouguer anomaly gradient.

A fairly constant regional gravity variation in the area was therefore assumed and by inspection of the Bouguer gravity profiles the regional trend was fixed for each profile (Fig 6.1). The residual anomalies were then

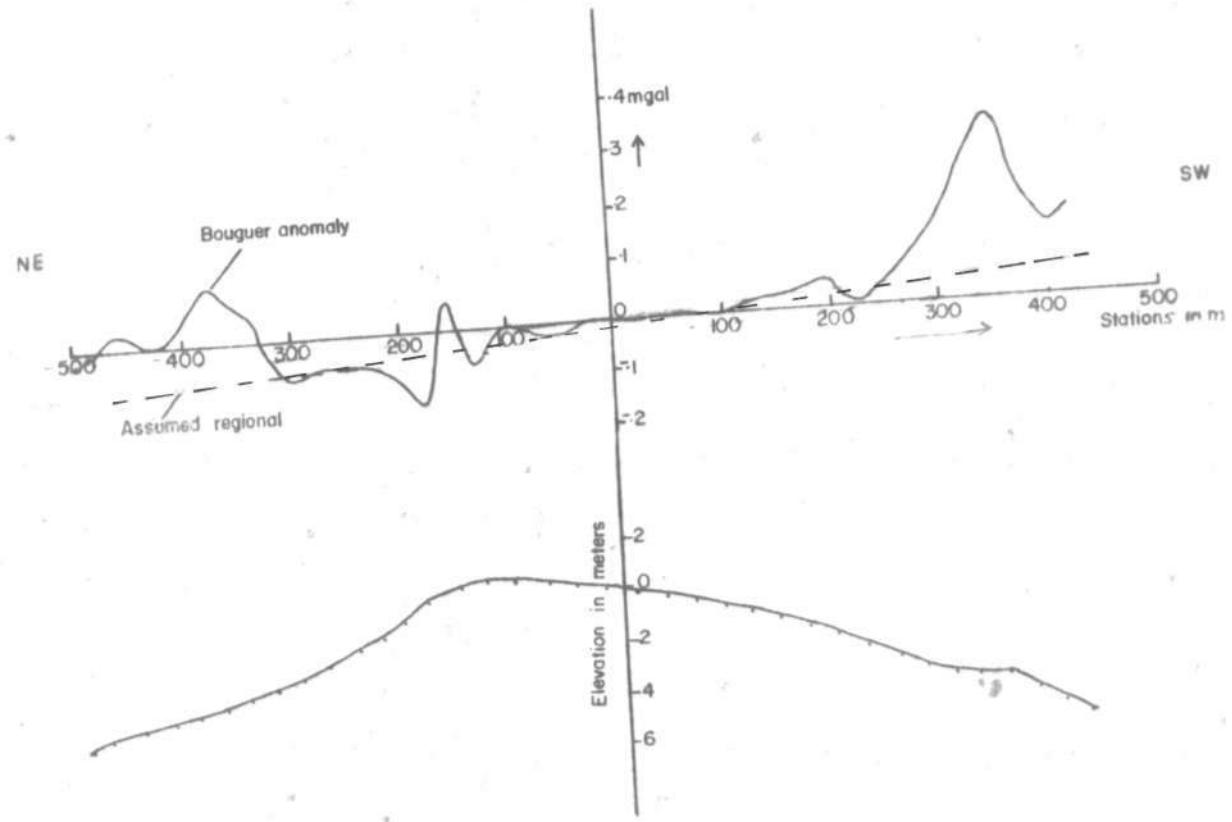



Fig 6.1 a Bouguer anomaly along profile II

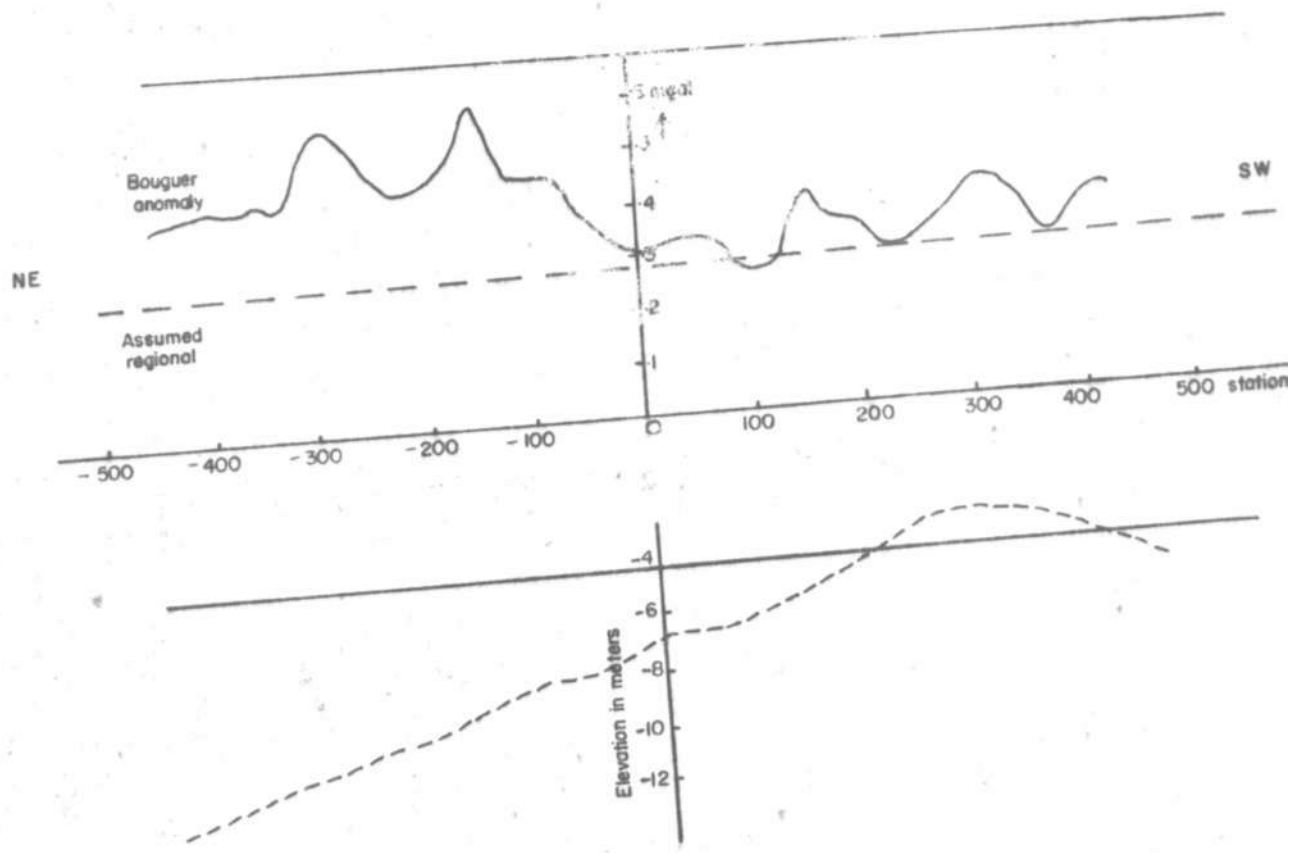



Fig. 6.1 b Bouguer anomaly along profile V

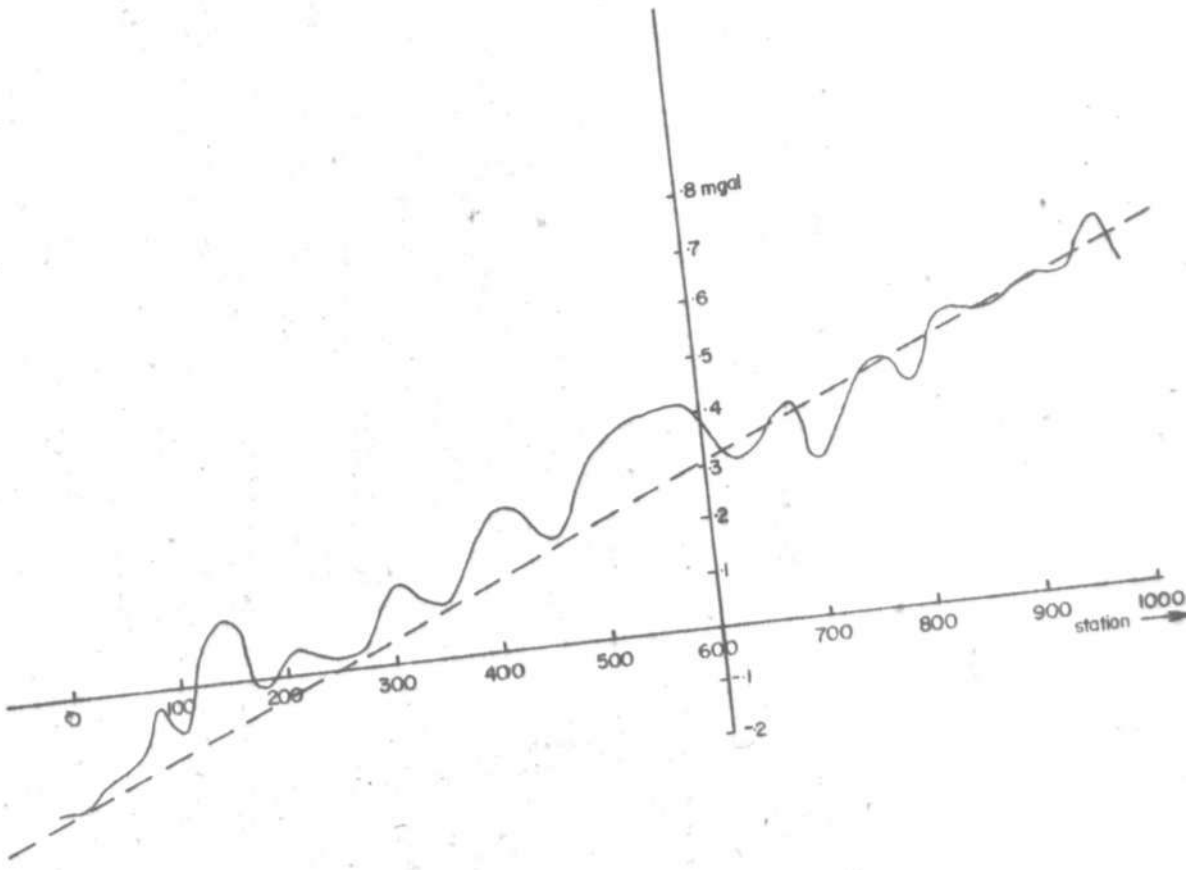



Fig. 6.1c Bouguer anomaly along profile VII

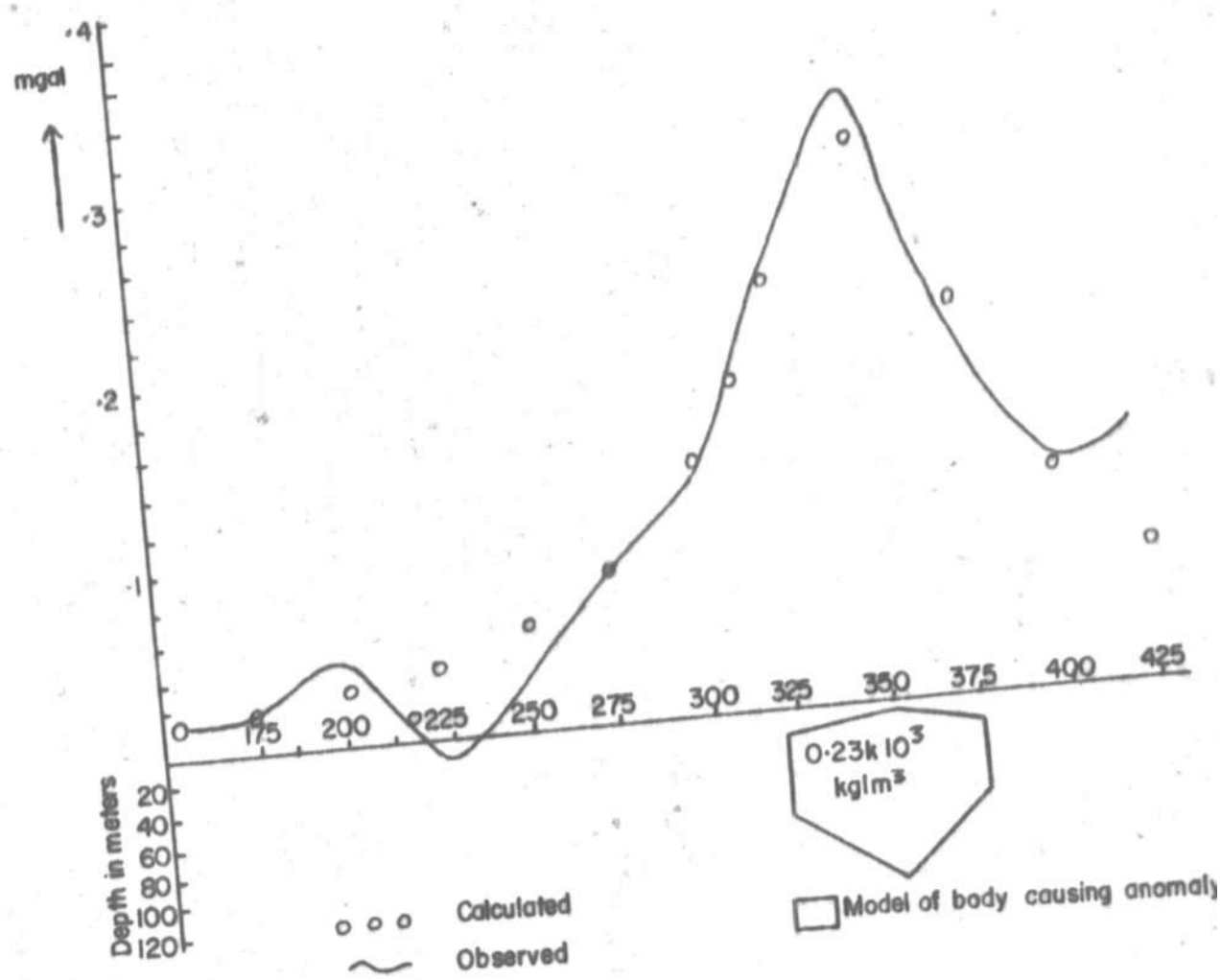



Fig. 6.2 Two dimensional model for the anmaly SW of profile II

obtained by subtracting the regional values from the observed at each station.

Positive residual anomalies of any significant value occur in the north-east (0.17 mgals) and south-west (0.37 mgals) of profile II and also to the north-east of profile V (0.3 mgals). On considering the relative positions of the anomalies in the geological map (Fig 2.2) it was discovered that the two positive residual anomalies NE and SW of profile II correspond nearly to the positions of two fault zones. The dip angles of the faults as revealed by drilling are $55^{o}$ and $60^{o}$ respectively. A fault with such an angle is characterised by a positive maximum and negative minimum gravity anomaly (Geldart et al, 1966). Since the anomalies under consideration are all positive it was regarded as an effect of a body with a high density contrast existing within the fault zones.

The first attempt at quantitative interpretation was to find the parameters of such a body. From table 6.1 the only rock type with density higher than that of shale which is the predominant rock is limestone. In chapter V it was suggested that calcium bi-carbonate in solution

can infiltrate into a fault zone. It is possible too that subsequent regeneration and evaporation can lead to a reasonable deposit of limestone. Such a deposit in a fault zone will follow the fault line. On this basis a dyke-like structure was modelled using the density contrast between shale and limestone.

A two dimensional gravity interpretation computer programme described by Nagy (1964) and adopted for use on HP 9830A mini-computer and plotter belonging to the Physics Department (Ojo,"personal communication") was used in the modelling. The programme uses the polygon approximation method of determining the gravitational attraction over a cross-section of a polygonal body which extends infinitely in a direction perpendicular to the cross-section.

In actual modelling the calculated values obtained from a hypothetical set of bodies extending into the subsurface with different shapes and a density contrast of $0.23 \times 10^3$ kg/m$^3$ with the surrounding host rock were plotted directly by the plotter on an overlay of the residual values for easy comparison. When the differences between the observed and the calculated were found to

be small, the model constituted a possible representation of the mass distribution.

The model of the body and calculated values superimposed on the residual values for the anomaly south-west of profile II is shown in Fig 6.2. It is about 50 meters wide and extends from a depth of about 20 meters to 100 meters. It is known that some faults in Obi are infact associated with $CaCO_3$ (limestone) (Okeudo,"personal communication") but the size of the body required to obtain a good fit in the modelling is not consistent with the present available geological information. More drilling in the area may throw some light on this problem. Models based on the same procedure was constructed for the other anomalies and the conclusions from the results are similar to the above.

The second approach was to try to determine any possible fault structure that could fit the anomaly.

The results of Geldart et al also show that the maximum or minimum gravity anomaly associated with a fault gradually disappears as the angle of dip of the fault approaches $15^{\circ}$ and less. The other condition under which the maximum or the minimum disappears for a normal or

reverse fault respectively, in addition to a small dip is for the top of the faulted bed to outcrop or be shallow and near the surface.

The positve anomalies therefore suggest a shallow reverse fault with a dip of less than $15^{o}$. The dip is not consistent with the geological information but the relatively high density beds which consist predominantly of shale has been shown in the resistivity chapter to be shallow (1-6 m). It is however pertinent to note that the curves described by Geldart et al is valid only for horizontal beds whereas the shale beds are slightly dipping in the survey area. It would therefore appear that the anomalies may tentatively be explained by reverse faults with the positive anomalies caused by the displaced shale beds.

# CHAPTER VII

## RESULTS AND CONCLUSIONS

### 7.1 Results from the various methods

Vertical electrical soundings (VES) in Obi coal-field indicate that there is a highly conductive section below an overburden of high resistivity of about 30 to over 2500 ohm-meters. Within the conductive section there exists two subsections with different resistivities. The first consists principally of shale having resistivity of 6 to 14 ohm-meters. The second is made up of interbedding of different rock-types with resistivity of 15 to 30 ohm-meters. Results further show that thick coal beds form part of the latter. VES have marked out the anticlinal structure within the survey area and given indications of two faults at the sounding points N and G. Resistivity profiling and VES have also indicated a third fault. VES curves confirm what was predicted by the theoretical and model resistivity curves especially for the zone containing many coal beds. This zone is easily recognised on the broad K-type curves.

The negative SP anomaly which occurs over a fault zone has been interpreted in terms of calcium bi-carbonate solution within a fault zone and the positive SP as an elevation effect.

Gravity measurements show that Bouguer gravity variation is low except for a few highs not exceeding 0.6 mgals. Two of such highs correspond with two faults predicted by drilling results.

There is agreement on the fault indicated along profile V between the three methods. However the other two faults NE and SW of profile II over which occurred gravity highs were not picked by resistivity profiling. This might be due to the constant electrode spacings used. Minor foldings and local inhomogeneities could have rendered the use of the particular electrode spacing inadequate for profiling work in the area. On the other hand varying electrode spacings from profile to profile might present problems in correlating the results.

## 7.2 Conclusions

This study can be considered as a preliminary investigation of the applicability of some geophysical methods in tracing coal-beds and in determining faults

in a coalfield in Nigeria. It is also a follow-up of the work of the N.S.D.A. in the area. Lack of adequate literature especially on self-potential method was among the problems encountered in the survey. Inspite of the usual difficulties inherent in the interpretation of geophysical data the following conclusions have been drawn from the results of this study:-

(a) A geological zone with resistivity ranging from 15 - 30 ohm-meters exists within a shale zone of resistivity of under 15 ohm-meters and contains most of the coal seams within the survey area. Wherever this zone is encountered its position and thickness will offer a useful control as to the depth to be drilled when prospecting for coal in the area.

(b) VES is generally useful in mapping out structures.

(c) Gravity and Self-potential gave results indicating fault structures.

(d) A very useful contribution of this study is the detection of the zone with resistivity of 15 - 30 ohm-m.

## 7.3 Recommendations

The profiles should be extended beyond the present limits especially northwards for the resistivity profiling. The profile intervals should be reduced to about 100 m for more detailed information, and resistivity soundings made on a more regular grid with sounding points located at 100 m from one another. This may help to indicate sharp discontinuities in the geoelectric section.

This should be followed up by SP measurements at closer station spacings than was used in the present survey especially near anomalies in order to further investigate its applicability in more detail in determining structures and in detecting coal zones. Gravity measurements can then be made at selected locations with suspected faults. More profiles for gravity measurements should also be established in order to determine the continuity of the anomalies and also a more detailed quantitative treatment of fault model should be carried out to check the results.

Seismic method is also recommended to be used since it can map out structures.

## REFERENCES

Auber, R.D., and Kopper W., 1976.
Paper read at the 25th International Geological Congress Sydney Australia

Bhattacharya, P.K. and Patra, H.P., 1968.
Direct current geoelectric sounding Elsevier Amsterdam

Clark, Sydney P. Jnr., 1966.
Handbook of Physical constants Geological Society of America

Cratchley, C.R., and Jones, G.P., 1965.
An interpretation of the Geology and gravity anomalies of the Benue Valley, Nigeria Overseas Geological Surveys Geological Paper No. 1.

Dobrin, M.B., 1976.
Introduction to Geophysical Prospecting McGraw Hill Book Company New York.

Garland, George D., 1971.
Introduction to Geophysics W.B. Sanders Company, Toronto, Philadelphia.

Geldart, L.P., Denis, E.G.U., and Bijon Sharma, 1966.
Gravity anomalies of two-dimensional faults. Geophysics Vol. xxxi No. 2,pp. 372 - 397

Grant, F.S. and West, G.F., 1965.
Interpretation Theory in Applied Geophysics McGraw Hill Book Company, N.York.

Johansen, H.K., 1975.
An iteractive Computer/Graphic Display-Terminal System for Interpretation of Resistivity Soundings. Geophysical Prospecting Volume 23.

Van Norstrand, R.G. and Cook Kenneth L., 1966

Interpretation of Resistivity Data
United States Government Printing Office
Washington.

Nagy, O., 1964.

The gravitational effect of two-dimensional masses of arbitrary cross-section
Publishing Gravity Division Ottawa

Offodile, M. 1976.

Geology of the Middle Benue
Ph.D. thesis University of Upsalla

Parasnis, D.S., 1975.

Mining Geophysics
Elsevier New York.

Paul, M.K., 1965.

Interpretations of self-potential anomalies due to Localised Causative bodies
Geophysics Vol. 61.

Reyment, R.A., 1963.

Aspects of Geology of Nigeria
Ibadan University Press.

Sears, F.W. and Zemansky, M.W., 1970.

University Physics, Addison-Wesly Pub. Co.

De Swardt, A.M.J. and Casey, O.P. 1963.

The Coal Resources of Nigeria, Geological Survey of Nigeria, Bulletin No. 28.

Verma, R.K., Majundar, R., Debabrata Ghosh, Ghosh Ashish and Gupta, N.C., 1976.

Results of Gravity Survey over Raniganj Coalfield, India.
Geophysical Prospecting Vol. 24 No.1 pp. 19 - 30.

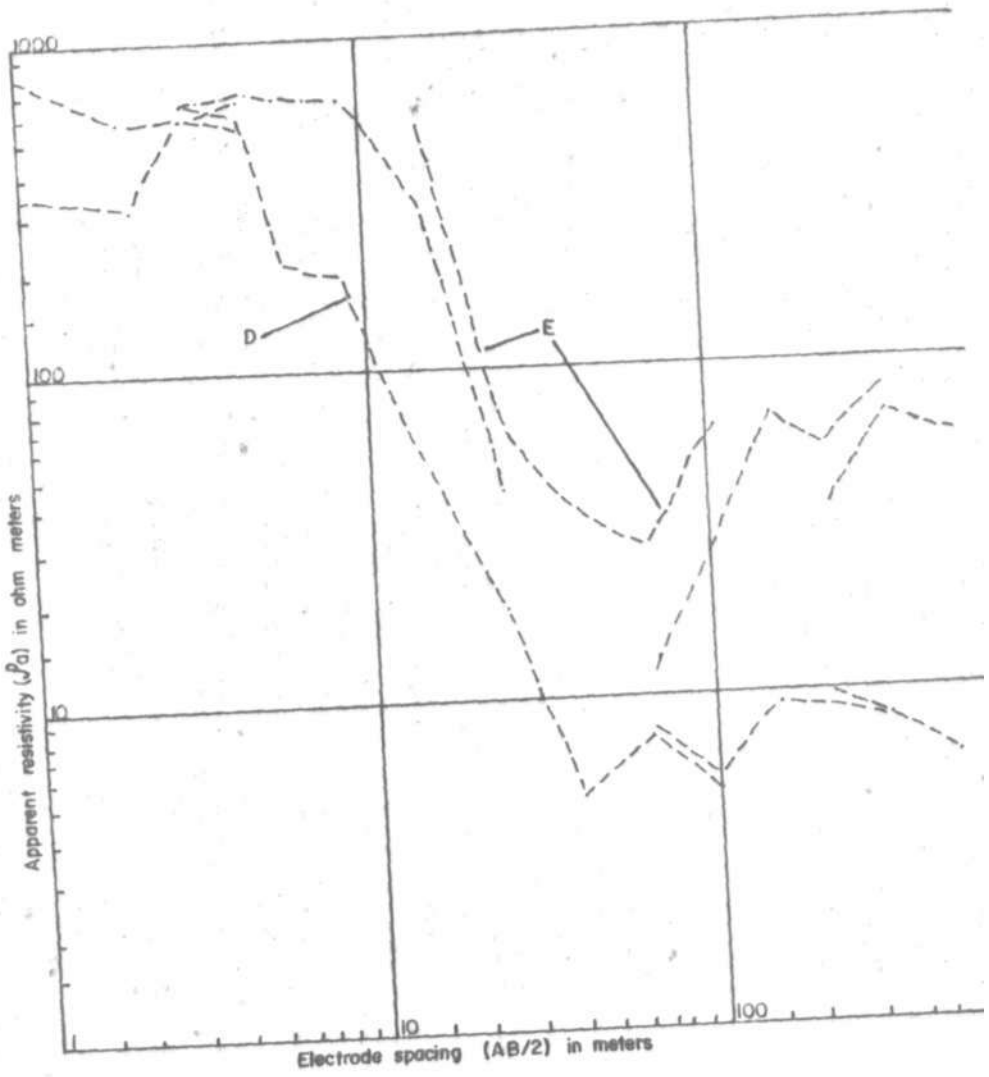
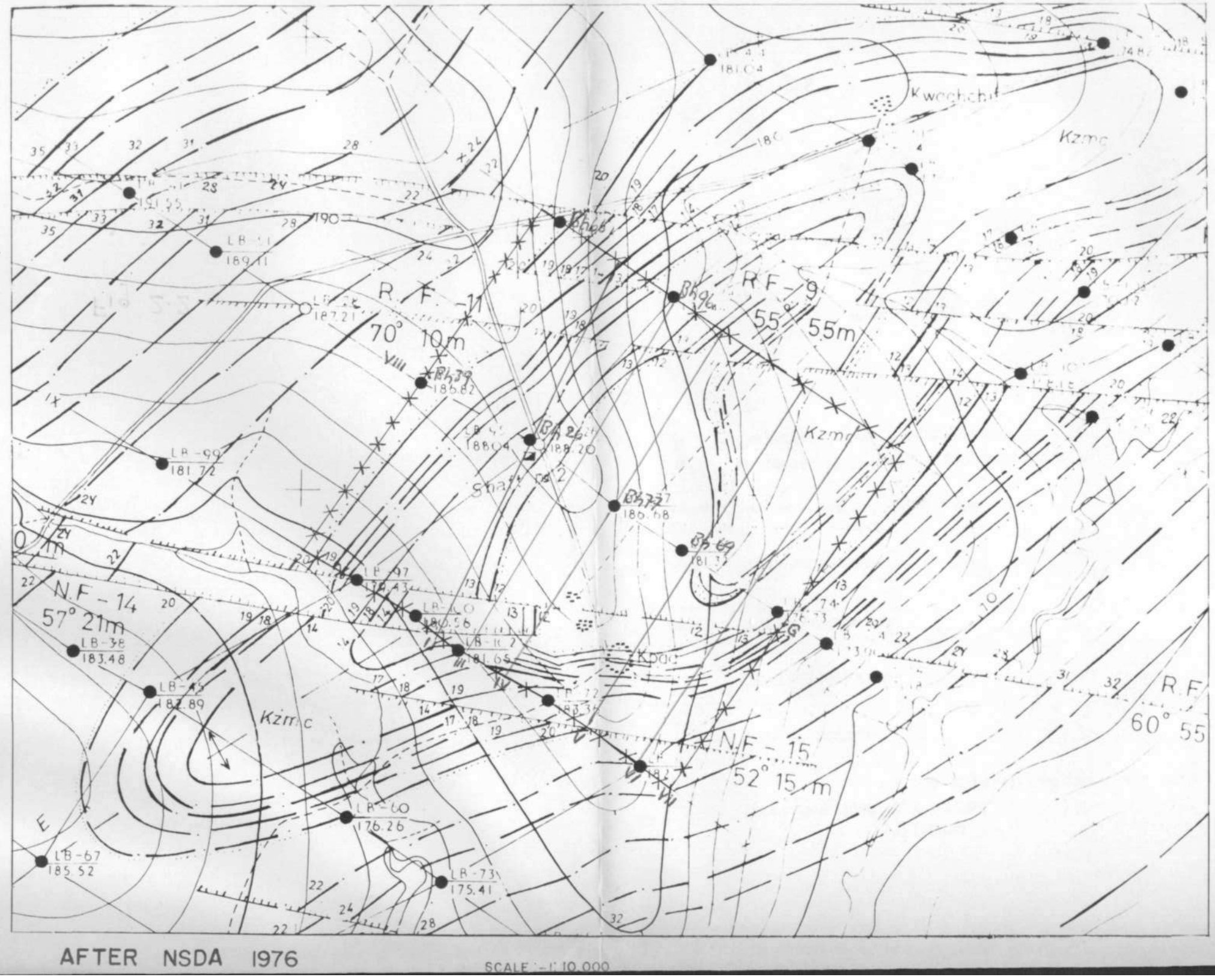



Fig 1. Resistivity plots with electrode spread across the strike of the anticline.

GEOLOGICAL MAP OBI AREA

PART OF LAFIA COAL DEPOSIT



100 0 100 200 300 400m

## EXPLANATION

- Predicted coal seam occurrence of the workable thickness.
- Predicted subsoil coal seam occurrence of the non-workable thickness.
- Predicted subsoil coal seam occurrence (non-prospected
- Predicted sandstone occurrence
- 15° 110° Anticlinal axis and dip angle of fold
- Synclinal axis
- Boundary between formations and measures
- Project Area

- Disjunctive fault. a) proved b) predicted c) dip angle of fault plane and throw — 70°25'
- iv —— iv Line of section
- kla Lafia sandstones
- kmz Argillite measures
- ktz Transitional layers
- kzmc Maximum coal bearing zone
- ● Boreholes drilled during detailed prospecting
- o Boreholes drilled during search.

Fig 2·2

GSN. 2128